Water resource management plan

Ground deformation monitoring and management program

AE-E

Enter ▶ Go back to contents ▶

CSG Fields Ground Deformation Monitoring and Management Plan

Santos
GLNG Project

Table of Contents

Santos
GLNG Project

1. Context of this Subsidence Management Plan

1.1. Regulatory Context

Santos Project Approval by the Department of Sustainability, Environment, Water, Population and Communities (SEWPaC) under the Environment Protection and Biodiversity Act (EPBC Act, 1999) warrants the approval to develop, construct, operate and decommission the CSG Fields conditional to a number of conditions.

This subsidence management plan addresses the conditions relating to the potential for CSG extractions to result in ground subsidence. This corresponds to Conditions 65 and part of Condition 69 as reported in Table 1-1.

Table 1-1 : Subsidence Requirements set in the Project Approval Conditions

Project Approval Condition	Condition
Condition 65 (a)	Baseline and ongoing geodetic programs to quantify deformation at the land surface within the proponent's tenures. This should link from the tenement scale to the wider region across which groundwater extraction activities are occurring and any relevant regional program of monitoring
Condition 65 (b)	Modeling to estimate the potential hydrogeological implications of the predicted surface and subsurface deformation
Condition 65 (c)	Measures for linking surface and subsurface deformation arising from CSG activities
Condition 69 b VI 2)	Within 12 months of the survey completion, provide to the Minister, a management plan for all relevant springs which includes special mechanism to avoid , minimise and manage risks, and response actions that can be taken by the proponent where subsidence or surface deformation occurs, particularly if it impacts on surface or groundwater hydrology

1.2. Definition of Subsidence, Process of Subsidence in the Context of CSG Production

Subsidence is the motion of a surface (usually, the Earth's surface) as it shifts downward relative to a datum such as sea-level. The opposite of subsidence is uplift, which results in an increase in elevation. Subsidence can have a number of causes such as dissolution of limestone (karstic systems) or dissolution of soils by fluid flow in the subsurface, underground mining activities, petroleum extractions, elastic deformation owing to groundwater level fluctuations, or be related to geological events such as earthquakes.

To facilitate the extraction of coal seam gas (CSG) from a gas field, it is necessary to reduce the initial pressure in the producing coal seams. Under natural conditions, the water pressure in the coal seam also supports the soil layers above the producing coal seams. As depressurisation of the coal seams proceeds, gas desorption commences and the combined water and gas pressure in the fractures and pores is reduced, there will be an increase in the vertical effective stress (i.e. the stress that is carried on the rock skeleton due to the weight of the overburden to the surface). An increase in the vertical effective stress will result in settlement of those formations. This has the potential to lead to subsidence at the ground level.

The level of subsidence is directly proportional to the thickness of the depressurised formations, the thickness of the overburden and the reduction in coal seam pressure. Propagation of subsidence from the CSG beds to surface depends on a number of factors including the thickness of the overburden and pressures within the formations.

Estimation of the amount of settlement and risks to ground surface and hydrology network are discussed in the next section.

2. Predicted Subsidence Levels & Subsidence Risk Levels

2.1. Predicted Settlement

The level of settlement is calculated for the formation depressurised. If multiple coal seams are depressurised, as will be the case for the Santos gas fields, there is potential for the interburden formations to also be depressurised.

The extent to which inter-burden formations are depressurised will depend on the spacing between the coal seams that are depressurised and the hydraulic properties of the inter-burden (hydraulic conductivity and specific storage). For the cases currently under consideration, the inter-burden layers are of the order of several tens of metres in thickness, and over the period in which the coal seam will be depressurised it is reasonable to assume that the inter-burden layers will be depressurised to the same extent as the coal seams.

According to the linear elastic theory, compression ΔZ of a given geological formation resulting from an increase in effective vertical stress within that formation is given by:

$$\Delta Z = Z_1(P_{i2} - P_{i1})/E$$

Where: Z_1 = thickness of the formation prior to compression;
P_{i2} -P_{i1} = change in pore pressure resulting from depressurisation (equal to the increase in vertical effective stress); and
E = Young's Modulus

In the case of underground coal mining, the settlement that is experienced at surface is generally less than that experienced at depth. This depends on a number of factors such as the depth and width of the extraction zone. Experience from underground coal mining indicates that about 60% of the coal thickness extracted may reach the surface as subsidence for depths of typically up to about 500 m. In these cases the reduction in surface settlement in relation to the settlement that occurs at depth is a result of the limited width of workings in relation to the depth. For smaller workings or greater depths the settlement at surface will be less, and for larger workings or shallow depths the settlement at surface will be greater, as a proportion of the settlement at depth. The mechanisms of arching and stress re-distribution in the overburden that takes place and that lead to a reduction in surface settlement may also have the potential to induce fracturing in the overburden.

In the case of CSG development, depressurisation will occur over a slightly wider area than the CSG fields themselves, because of the lateral extent of groundwater drawdown in the coal seams. This infers that settlement, too, will occur over a broader area than the footprint of the CSG well field. There is little or no potential for a reduction in surface settlements through arching or similar mechanisms in depressurised CSG fields because the areas outside the area of greatest drawdown (i.e. the area of the CSG wells themselves) are subject to compression.
The magnitude of compression that occurs at depth in the coal measures is likely to be closely reflected at the surface, however, the stresses and strains induced in the overburden will be significantly lower than in the case of underground mining because of the broad extent of settlement and shallow gradients of settlement. It is therefore far less likely than for mining that settlements induced by depressurisation could lead to fracturing of overburden materials and therefore cause an increased interconnection between the coal measures and overlying aquifers.

The change in pore pressure, and therefore assessment of subsidence, resulting from depressurisation and used to estimate compression across the Santos GLNG CSG fields has been derived from the UWIR (see Section 5.1). Note that these calculations do not consider the impacts of compartmentalisation of coal seams. Where compartmentalisation exists it is likely to reduce potential subsidence impacts from coal seam water extraction.

Roma CSG field

The Roma CSG field targets the Walloon Coal Measures and this coal measure sequence is on average approximately 300 m thick (25 m thickness of coal seams, and 275 m thickness of other sedimentary rocks).

A maximum 'all time' drawdown of approximately 700 m is predicted in the Walloon Coal Measures. Extraction will take place from up to 12 coal seams. As indicated above, because of the limited thickness of sedimentary inter-burden layers, it has been assumed that the full 300 m of coal measures is depressurised.

A rock mass modulus of 2 GPa is assumed for the coal seams. 10 GPa is assumed for the remainder of the formation.

For an average drawdown of 700 m of head, the calculated subsidence for the Walloon Coal Measures is as follows:

- 0.08 m for the coal seams;
- 0.20 m for the remaining thickness of the formation; and
- Total of 0.28 m.

Fairview and Arcadia Valley CSG fields

The Arcadia Valley and Fairview CSG fields target the Bandanna Formation. This formation is approximately 100 m thick with 10 m thickness of coal seams, and 90 m of other sedimentary rocks.

A maximum 'all time' drawdown of approximately 1,000 m is predicted in the Bandanna Formation. This figure was assumed to apply to both coal seams and other sedimentary rocks in the Formation.

A rock mass modulus of 2 GPa is assumed for the coal seams. 10 GPa is assumed for the remainder of the formation.

For an average drawdown of 1,000 m of head, the calculated subsidence for the Bandanna Formation is:

- 0.05 m for the coal seams;
- 0.10 m for the remaining thickness of the formation; and
- Total of 0.15 m.

2.2. Hydrological implication for the predicted settlement

As indicated previously, it is likely that these settlements would be very closely reflected at surface. There is potential for strain to be induced in the overlying formations due to differential depressurisation, and consequently differential compression, of the coal formations. In principle, these strains will have the potential to influence the overlying formations.
The maximum gradient in settlement is calculated to be approximately 0.001% for Roma, i.e. a differential settlement of 0.2 m (70% of total drawdown) over a distance of 2 km from the edge of the CSG field and wholly depressurised coal seam.

The maximum gradient in settlement is calculated to be approximately 0.0005% for Arcadia Valley/Fairview, i.e. a differential settlement of 0.1 m (70% of total drawdown) over a distance of 2 km from the edge of the CSG field and wholly depressurised coal seam.

Arising from these very low estimates of subsidence, there would be negligible potential for impact on subsurface hydrology, Furthermore, because of the relatively small amount of predicted settlement and the extremely small differential settlement gradients, Santos GLNG considers that there will be no impacts on MNES as a result of subsidence induced by CSG production. Accordingly, there will be no impact on:

- The integrity of the Great Artesian Basin aquifers; and
- The quantity or quality of surface water flows in the Murray Darling Basin.

Notwithstanding the above conclusions, ground deformation and water level monitoring will be carried out to verify the above assumptions and the assessed risk.

2.3. Hydrogeological implications

The mechanisms of arching and stress re-distribution in the overburden that takes place and that lead to a reduction in surface settlement may also have the potential to induce fracturing in the overburden. However, arising from the very low estimates of subsidence, there would be negligible potential for impact on subsurface hydrology. As a consequence there will be no impact on the integrity of the Great Artesian Basin aquifers.

Notwithstanding the above conclusions, ground deformation and water level monitoring will be carried out to verify the above assumptions and the assessed risk.

3. Subsidence Monitoring

3.1. Method used for Monitoring subsidence

Santos GLNG is using InSAR (interferometric synthetic aperture radar) technology to detect ground movement and deformation across the entire extent of its CSG fields. InSAR is an aerial or satellite based radar technology used in geodesy and remote sensing. The method uses two or more synthetic aperture radar images to generate maps of surface deformation or digital elevation by analysing differences in the phase of the waves returning to the satellite. The satellite based geodetic survey is industry best practice and will identify cumulative subsidence for all contributing factors (agricultural extraction, seasonal variation, coal seam water extraction etc) to an accuracy of millimetres.

Radar imagery processing is the core competence of Santos GLNG's contractor, Altamira Information, who has been carrying out ground displacement analysis in the Santos GLNG CSG fields. Altamira Information has a track record working on ground displacement analyses for mining and oil and gas industries across the globe. It is also the reference InSAR provider for NASA (National Aeronautics and Space Administration), CSA (Canadian Space Agency), ESA (European Space Agency), JAXA (Japan Aerospace Exploration Agency), CNES (French Space Agency) and DLR (German Centre for Aeronautics and Space).

Altamira Information is the developer and the owner of the advanced InSAR technique Stable Point Network (SPN) which has a potential to increase the precision of measurements in space and time. InSAR technology can be based on a number of past, present and future satellites, making it possible to analyse past, current and future deformations and providing assurance for the continuity of the proposed approach into the future.

3.2. Baseline Results

Santos GLNG commissioned a baseline assessment which was undertaken between Q4 2011 and Q2 2012. The baseline assessment report can be found in APPENDIX A.

Altamira obtained between 13 to 24 satellite images (i.e. measurements) per track dating from December 2006 to February 2011 for the extent of the CSG fields in the Surat and Bowen Basins. This represented a total of 698 ALOS SAR images over an area of 55,000 square kilometres. The processing resolution of the images was of 35x35 metres, ground positioning of a point after a number of image corrections had a resulting precision of 10 m (i.e. the centre of the 35mx35m pixel is located within 10 m of its real location). High quality reflectance points were identified and used as radar stable points, this methodology is known as the Stable Point Network (SPN) methodology. The radar stable points are used to extract precise displacement and position information.

The baseline results detected no large scale ground deformation. Ground deformation is considered stable when the results are within +/- 8 millimeter per year (mm/year) of average annual displacement rate. This is the case for 97% of the baseline study area. Several areas with local patterns of deformation were detected. These deformations were related to natural or anthropogenic factors and are related to irrigation pools and ponds, rural roads, fields and riverbanks. Within these deformations, just 0.3% of the study area were areas of subsidence or uplift with a displacement rate higher than 15 mm/year, they were distributed throughout the study area and are not representative of a large scale or systematic ground motion.

The report from that assessment has indicated that high resolution and wide-swath SAR data can provide a solution to measure both localised and regional ground motion.

3.3. Ongoing Deformation Monitoring

The approach defined here is the same as for the rest of the Industry over the Surat and Bowen Basins. Altamira is engaged for a period of 2.5 years, with the first acquisitions in July 2012 to continue with InSAR monitoring across GLNG tenements. The current project will utilise Radarsat-2, and will acquire data every 24 days for the first year and then every 48 days thereafter. The frequency of data acquisition is based on the acquisition of a minimum set of images to perform the SPN processes. Data acquisition every 48 days ensures that coherence between images is maintained.

Average expected precision is expected to be in the order of 5 mm and 7 mm and the data will be at a spatial resolution of 30 m x30 m. Processed data will be delivered after 1 year and 2.5 years of acquisition.

Note: Although the approach is the same across the CSG industry in The Surat and Bowen Basins, Altamira will provide data individually to QGC, Santos, Arrow and APLNG over a spatial coverage defined by each company.

After one year of data collection (namely in Q4 2013), an interim review of the InSAR monitoring data will be undertaken within the following areas, on tenement:

- 20 km radius of EPBC species or community
- 5 km radius of all CSG production areas and reinjection areas
- 5 km radius of high population areas (i.e. the towns, including Roma and Wallumbilla)

3.4. Supporting Monitoring

Groundwater pressure monitoring is carried out throughout Santos GLG fields. Groundwater pressure data measured primarily from the coal seams, will assist in the interpretation of an impact if observed. Groundwater pressure data from other formations may also be used as required.

A number of geodetic points are located throughout the CSG fields. The ongoing monitoring of the elevation at these points is not part of Santos GLNG subsidence monitoring program. These points will be used in the management response process would a risk of impact be confirmed and require geodetic confirmation. Increased monitoring at selected points could also be part of managing the risk of subsidence in identified areas of subsidence.

4. Exceedance Management and Response Plan

Differentiation between CSG and non-CSG induced ground deformation will be possible through the analysis of the historic and ongoing InSAR measurements. Examples of non-CSG induced ground deformation may include:

- Erosional and depositional geomorphological processes
- Climatic effects on shallow soils (e.g. rainfall induced swelling and subsequent settlement)
- Anthropogenic land use changes, be they agricultural (e.g. ploughing and cropping), municipal (e.g. urban development, road building), or industrial (e.g. mining activities)
- Continental scale (e.g. tectonic) uplift or subsidence

4.1. Subsidence Trigger

A ground motion is defined as stable for deformation average annual deformation values contained between – 8 mm/ year and + 8mm/ year. Ground motions are defined as subsidence or uplift for average annual values higher than -16 mm/year and +16 mm/year respectively.

The processed data provided by Altamira will be quantitatively processed in a GIS environment (e.g. ArcGIS). A floating grid methodology will be used to evaluate areas of subsidence. The grid size of 1.5 km by 1.5 km was defined to match the grid size of the Surat UWIR model.

As identified during the baseline exercise localised subsidence or uplift can be the result of a natural event or a local installation. To remove those types of events from the analysis, Santos has defined the subsidence trigger as follows:

The subsidence trigger associated with CSG production (natural and anthropogenics non CSG effects removed) is defined as an annual average ground motion of 16 mm/year for over 50% of data points of a 1.5 km x1.5 km region.

Sixteen millimetres represents an average annual rate of change equal to twice the magnitude considered “stable” in the ground motion baseline. Should the analysis identify such areas, analysis of the cause of the ground motion will be assessed.

4.2. Response to Exceedance

The response process to a confirmed ground motion exceedance as defined above is illustrated on Figure 4-1 and discussed in the following paragraphs.

Should the subsidence trigger be exceeded, Santos GLNG will carry out an investigation to identify the process resulting in the exceedance. This will specifically involve looking at the location and timing of the deformation with respect to other factors such as:

- Nearby (localised) and far field (e.g. regional) ground motion data (e.g. review of other InSAR data)
- Land use changes and activities (e.g. as observed by ground staff, or through aerial photography) which may explain a change to the reflectance data or a local ground motion. For example, during the baseline, it was identified that roads and dams have the potential to create a local subsidence pattern. Agricultural practices can also influence the reflectance readings and may need to be confirmed for the exceeding area.
- Seasonal climatic conditions (e.g. comparison with weather data, identification of flood periods which may affect the reflectance measurements)
- CSG activities have the potential to create subsidence through the dewatering of the coal seams. Santos GLNG will assess the formation pressure monitoring data monitored through the CSG field groundwater monitoring program to confirm the presence and degree of depressurization in the underlying coal seams and possibly in some of the overlying formations.

The investigation will conclude if there is a risk that the exceedance is (or not) related to CSG activities. In case of inconclusive results a survey of geodetic points will be undertaken.

If the risk that the observed ground motion exceedance is regional and due to CSG activities, a risk analysis focusing on the risk and consequence of deformation on springs and hydrology networks will be carried out. The risk analysis may require additional assessments to understand fully site specific features such as site walkovers, detailed aerial photography, ground-based geodetic surveys and other environmental monitoring data may be commissioned to confirm the level of risk associated with the observed exceedance. An unacceptable risk will trigger the following:

- An assessment of mitigation options;
- An assessment of the timing of the long term impact; and
- If required, the development of a mitigation plan. The criteria and timing for implementation of the mitigation plan will be defined in the plan with full understanding of the potential risks to EPBC springs and hydrological network.

Santos
GLNG Project

Figure 4-1: Subsidence Exceedance Response Process

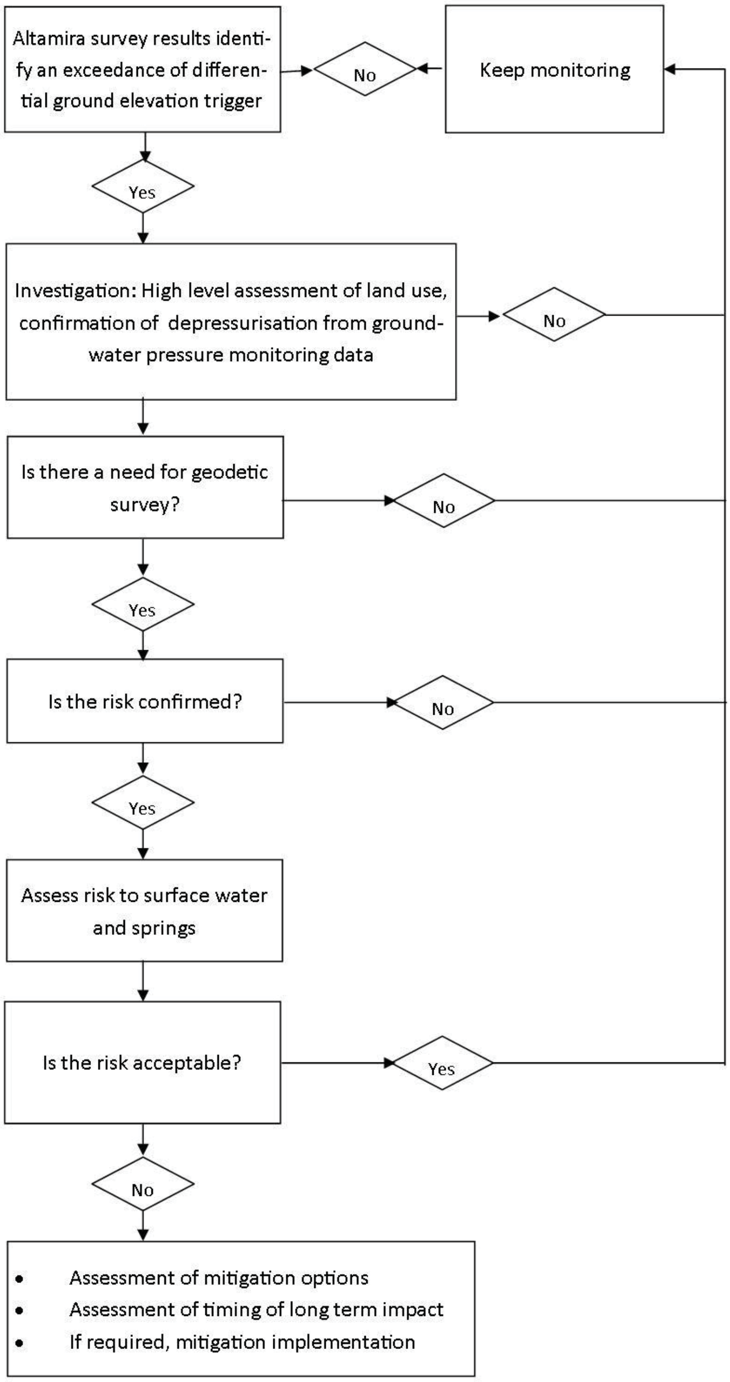

5. Reporting

An interim report on the ongoing baseline InSAR monitoring program will be prepared for SEWPaC that maps the average annual deformation measured by InSAR in each of the areas assessed at the end of the first year of data collection. Each ground motion exceedance that is determined to be real shall be clearly highlighted. Any further environmental monitoring, in addition to the InSAR monitoring, that is deemed appropriate will be clearly specified for each location.

Every five years, all ground motion data collected to date shall be reviewed, reported and analysed in respect of the risk of possible ground motion effect upon receptors such as:

- Surface water drainage
- Hydrogeology of aquifers (particularly source aquifers of springs that support EPBC species and communities)
- Surface infrastructure (buildings, roads, etc)

Where effects on such receptors are identified, the possible causes of deformation shall be identified, and an ongoing monitoring and management plan will be proposed that is tied back to an objective assessment of risk.

The following timetable for report submissions to SEWPaC is likely to be scheduled by the Ground Motion Monitoring and Management Plan.

Planned Submission Date	**Item / Report**
Q4 2013	Interim report on the ongoing InSAR monitoring program (ground motion between end of baseline (February 2011) and one year of collection of monitoring data.
July 2017 (every five years thereafter)	Five year ground motion report (reviews data from July 2012 to July 2017).

APPENDIX A: SUBSIDENCE BASELINE ASSESSMENT REPORT

Title: **BASELINE REPORT ON InSAR MONITORING ON THE SURAT-BOWEN BASIN**

Addressed to:

Authors: J. Duro, D. Albiol, J. Sabater

Approved by: B. Payas

Ref.: AI_051212_BASELINE_REPORT_01.pdf

Version: 01.1

Date: 05/12/2012

1. EXECUTIVE SUMMARY

This document presents the results of the study of the analysis of ground motion using InSAR technology conducted for Arrow Energy Pty[1], Australia Pacific LNG Pty (Origin), QGC Pty and Santos Limited in the Surat and Bowen Basins located in southern Queensland, Australia. This study has been undertaken in response to conditions imposed by the federal regulator for "*baseline and ongoing geodetic monitoring to quantify deformation at the land surface within the proponent's tenures*". The aim of this project was to establish a baseline of ground surface motion across the gas fields prior to the advent of significant CSG development.

Altamira Information's Persistent Scatterer Interferometry (PSI) technique, named Stable Point Network (SPN), was used for the study. The SPN technique has been applied in order to measure the ground motion for the period December 2006 to February 2011 using archive ALOS satellite SAR imagery. This involved the processing of 698 Synthetic Aperture Radar (SAR) images from seven different satellite tracks to cover the 55.000 Km^2 area of interest. Given the land cover characteristics of the site the density of measurement points is high, presenting an average of 600 PS/Km^2, except over agricultural fields where the number of measurement points is reduced due to the effects of the regular temporal changes.

This report presents a summary of the results delivered to Arrow Energy Pty, Australia Pacific LNG Pty, QGC Pty and Santos Limited for each of their specific areas of interest. The majority of the measurement points show stability (magnitude of ground motion below 8 mm/year) and do not show any apparent large scale deformation pattern. Nevertheless, many small patches of uplift and subsidence that were related to natural or anthropogenic factors can be found heterogeneously distributed throughout the study area.

Several areas showing deformation at a rate greater than 16 mm/year are identified and presented in this report. Some areas of ground motion are observed over different fields, in some cases very close to rural tracks. In many cases subsiding points are detected over the boundaries of ponds or irrigation pools. Also, uplift patterns can be seen over riverbanks, which might be caused by the significant rainfall events that occurred in 2010.

The use of high resolution and wide swath SAR data can provide an accurate, detailed, cost effective solution to measure local ground motion, but also enable monitoring of any motion on a regional scale.

[1] Arrow Energy not yet received federal government approval, and is not subject to these approval conditions at this time. However, at such time that federal approval of Arrow's project is approved, Arrow anticipates that federal conditions will be similar to those of the three approved projects.

INDEX

CHANGE RECORD FOR THIS DOCUMENT

Version	Date	Sections	Description of changes
01.0	12-07-2012	All	Creation of the document

ACRONYMS AND ABBREVIATIONS

ACR	Artificial Corner Reflector
ALOS	Advanced Land Observing Satellite
AOI	Area of interest
CR	Corner Reflector
CSA	Canadian Space Agency
Envisat	ENVIronmentalSATellite
ERS	European Remote Sensing satellite
ESA	European Space Agency
GPS	Global Positioning System
InSAR	Synthetic Aperture Interferometry
JAXA	Japan Aerospace Exploration Agency
SAR	Synthetic Aperture Radar
SPN	Stable Point Network
PSI	Persistent Scatter Interferometry

2. INTRODUCTION

Arrow Energy Pty[2], Australia Pacific LNG Pty (Origin), QGC Pty and Santos Limited are developing individual coal seam gas (CSG) to Liquefied Natural Gas (LNG) projects in the Surat and Bowen Basins in southern Queensland. This study has been undertaken in response to conditions imposed by the federal regulator for "*baseline and ongoing geodetic monitoring to quantify deformation at the land surface within the proponent's tenures*". The premise behind potential ground motion is that compaction of the geological strata may occur as formation pressures are reduced to allow CSG production, potentially resulting in surface subsidence. In order to satisfy these conditions the proponents have commissioned a study to baseline possible ground surface motion across the gas fields prior to the advent of large scale CSG development.

ALTAMIRA INFORMATION performed this ground motion baseline study utilising Interferometric Synthetic Aperture Radar (InSAR) technology on behalf of the consortium of companies. This document presents a summary of the method used and results of the baseline study. The main objective of this project was to establish a baseline of ground motion over the area of interest for comparison with ongoing surface deformation monitoring during approved CSG developments.

Synthetic Aperture Radar (SAR) data was acquired and processed through the application of Persistent Scatter Interferometry (PSI) techniques to natural radar reflectors. ALTAMIRA INFORMATION'S Stable Point Network (SPN) software was used in order to measure the ground motion for a period of over four years (December 2006 to February 2011) using historical ALOS satellite imagery. The analysis over the area allowed the retrieval of more than 30 million measurement points which represent a mean density of about 600 PS/Km^2.

A description of the area of interest and the parameters of the ALOS acquisitions used are shown in Sections 3, 4 and 5. Section 6 details an explanation of the methodology used to measure the ground motion, namely the Stable Point Network (SPN) technique. Section 7 describes the products delivered to the consortium.

The results of the application of the technique and the resulting measurement of the ground motion in the area of interest are presented in Section 8. Finally, the conclusions of the project are discussed in Section 9. Appendix A offers an interpretation of the measurements collected for specific areas where ground motion was noted. Appendix B shows a comparison of the results with the historical rainfall data over some particular areas. Appendix C offers an analysis of the impact of reflectivity changes over fields.

---

[2] Arrow Energy not yet received federal government approval, and is not subject to these approval conditions at this time. However, at such time that federal approval of Arrow's project is approved, Arrow anticipates that federal conditions will be similar to those of the three approved projects.

3. AREA OF STUDY

The study area is located in southeast Queensland, and is underlain by the Surat and Bowen geological basins. The study area has been defined by the individual proponents based on their relevant petroleum tenements (see Figure 1) and in some cases, additional area of interest adjacent to and outside of the tenements. The study area covers approximately 55,000 Km².

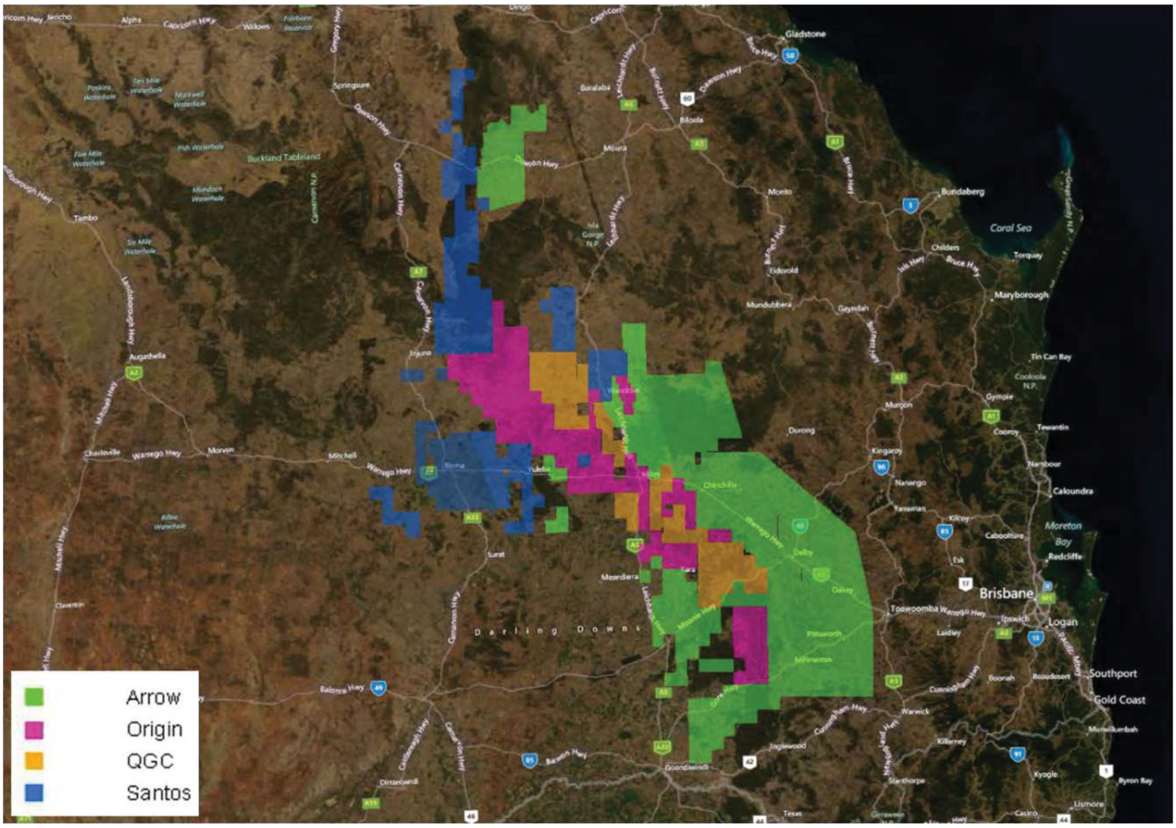

Figure 1: Location and Extent of the Study Area.
(© Bing Maps 2010 Microsoft Corporation orthoimage)

With respect to the land cover characteristics of the site, the terrain is mainly rural, composed of agricultural fields and forests, with few manmade structures and those existing are mostly located over small populated areas. As an illustration example, Figure 2 shows an orthophoto of a small sector within the area of study representing generalized landcover found in the rest of the area of study. The agricultural field patterns are clearly visible in the centre of the orthophoto as well as highly vegetated zones and forests on the bottom left corner of the image. This can be confirmed by looking at the landcover map of the same area (middle image), where crops, pasture and terrestrial vegetation are predominant over the specified areas.

The maps were obtained on the National Dynamic Land Cover Dataset of Australia from the Australian Bureau of Agricultural and Resource Economics and Sciences (c) webpage.

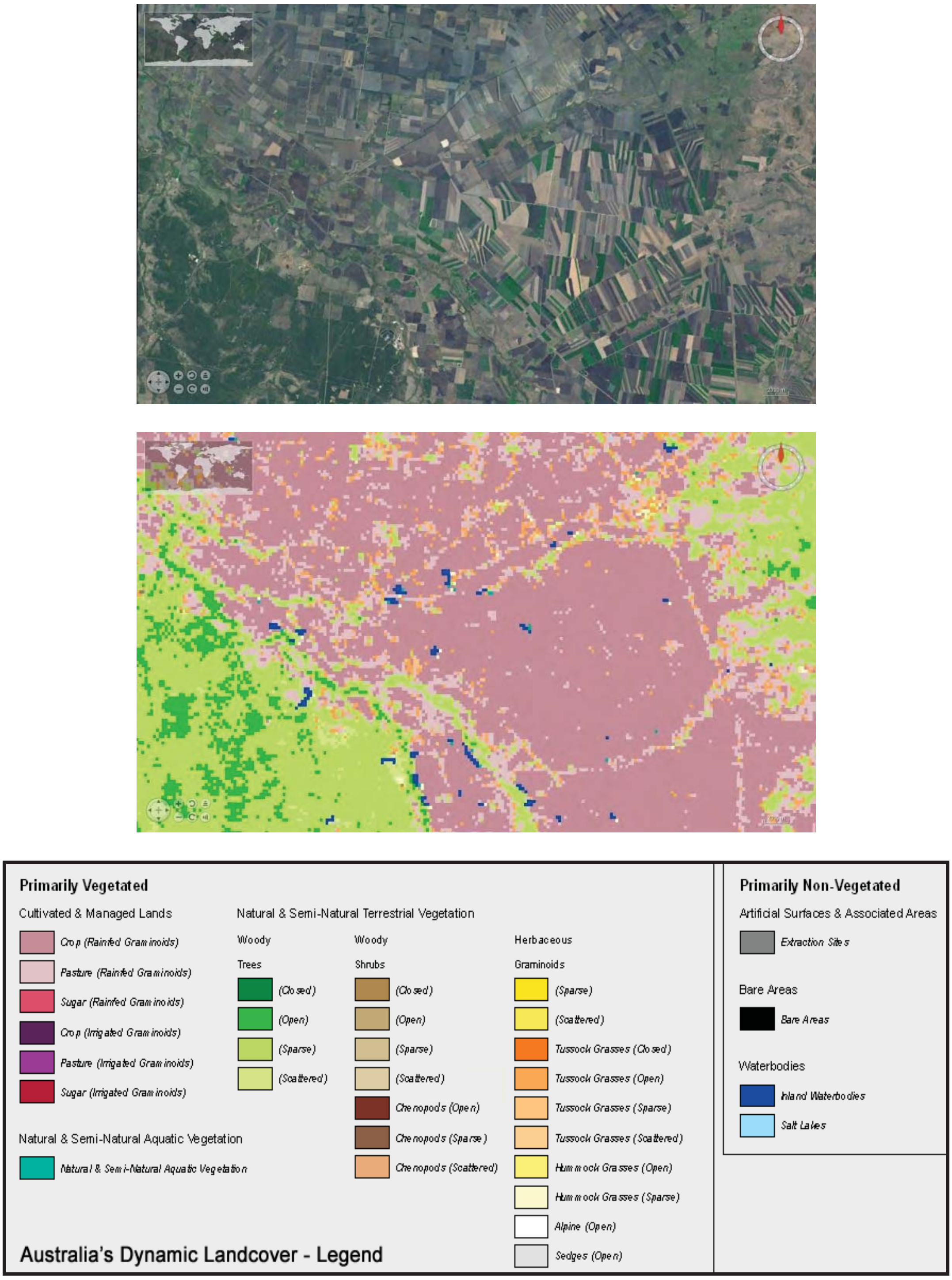

Figure 2 : Orthophoto and landcover indicative of landuse across the study area

4. SAR DATA USED

4.1. JUSTIFICATION OF THE SATELLITE SELECTION

ALOS satellite (showed in Figure 3) was launched by the Japanese Aerospace Exploration Agency (JAXA) on January 2006. Among other sensors on board, the satellite contains a phased array type L-band synthetic aperture radar (PALSAR) which allows providing resolution images of 4.5m x 5m with the fine beam single polarization mode with a maximum interferometric revisit time of 46 days.

One important characteristic of this Japanese SAR mission is that it has a background acquisition mode which gives the opportunity to look into the recent past. This background mode system makes it possible to have acquisitions over certain areas without programming the satellite. As a consequence, good stacks of data are available in order to perform historical ground motion studies.

In particular, the available data archive provided by this mission over the whole area of interest was very uniform in comparison with the data archive given by other missions like ENVISAT. ALOS mission provided of about 20 acquisitions over time (between 2007 and 2010) with a complete coverage of the area of interest. Meanwhile, ENVISAT mission data archive presented an unevenly time distribution of the images in space and time. For example with an stack of 30 images over time in some areas and only 10 in other location, which represent an insufficient number of images to perform a InSAR analysis for ground motion measurement.

Satellite	ALOS
Band	L
Frequency	1.2 GHz
Wavelength	23.6 cm
Look angle	10º – 50º

Figure 3 : Advanced Land Observation Satellite (ALOS)

Another important characteristic of the ALOS PALSAR images is the good compromise given between the coverage and the resolution. The image frames have an approximate coverage of about 70x70 Km at a resolution of 5x5 meters approximately. Due to the large extension of the area of interest, the selected dataset includes 34 different ALOS frames, each containing a range of images which varies from 13 (minimum) to 24 images, with an average of 20 images per frame.

The final important characteristic of this sensor which justifies its selection among the other for the historical motion analysis is that it works in L-band (against the C-band of ENVISAT). L-band data gives higher coherence than C-band data in rural environments. Compared with the other sensors available for the historical analysis, ground deformation maps produced with the ALOS data are less affected by the temporal changes which could occur during the period of analysis in such type of areas (crops, fields, forest, flooding, ..). The ground deformation maps have a uniform distribution of the measurement points through the whole AOI minimizing as much as possible the local areas without measurements.

4.2. DATA ACQUIRED

The ALOS datasets used in this study correspond to the ascending tracks 364, 365, 366, 367, 368, 369 and 370, which completely cover the areas of interest as seen in Figure 4. The period of study was from December 2006 to February 2011. This configuration of SAR acquisitions represents the best availability of archived data to analyse the past motion in terms of coverage and available number of acquisitions for this site.

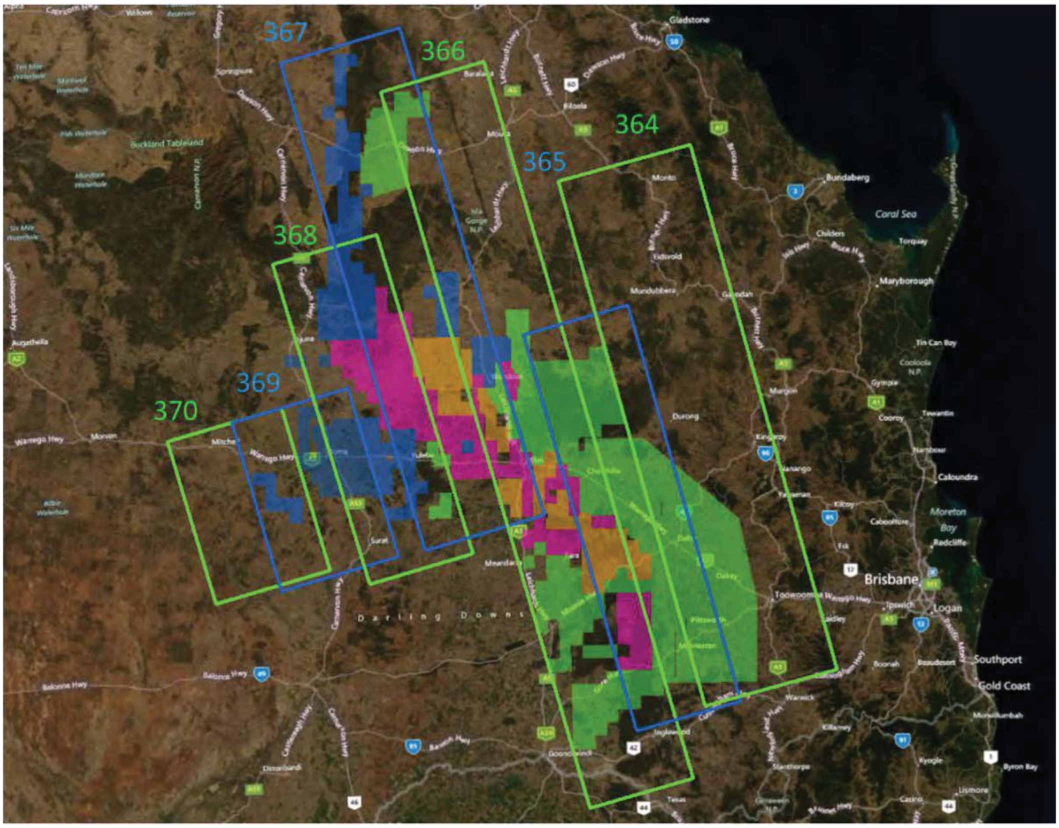

Figure 4: Coverage of the areas of interest with ALOS ascending tracks 364, 365, 366, 367,368, 369 and 370. Note that each track has several frames

Each track represents a long strip of data composed by several frames; the approximate coverage of these tracks is presented in Figure 4. It is important to point out that each track represents a satellite pass (or date of measurement). The tracks have a small area of overlap between them but they have been acquired at different dates.

Table 1 summarizes the main parameters of the stack of ALOS datasets acquired over the period of study.

Satellite	Track	Orientation	Images per frame	Frames per track
ALOS	364	Ascending	24	4
	365	Ascending	20	5
	366	Ascending	22	9
	367	Ascending	20	7
	368	Ascending	21	5
	369	Ascending	13	3
	370	Ascending	20	1

Table 1: ALOS data archive per track. Each track has a different number of frames making a total of 698 SAR images used.

The following tables (2 to 8) present the acquisition dates and orbit number processed for each of the tracks.

	Acquisition date	Orbit number			Acquisition date	Orbit number
1	01-02-2007	5447		13	22-12-2008	15512
2	19-06-2007	7460		14	09-08-2009	18867
3	04-08-2007	8131		15	24-09-2009	19538
4	19-09-2007	8802		16	09-11-2009	20209
5	04-11-2007	9473		17	25-12-2009	20880
6	20-12-2007	10144		18	09-02-2010	21551
7	04-02-2008	10815		19	27-03-2010	22222
8	21-03-2008	11486		20	12-08-2010	24235
9	21-06-2008	12828		21	27-09-2010	24906
10	06-08-2008	13499		22	12-11-2010	25577
11	21-09-2008	14170		23	28-12-2010	26248
12	06-11-2008	14841		24	12-02-2011	26919

Table 2: ALOS track 364 data archive constitution.

	Acquisition date	Orbit number		Acquisition date	Orbit number
1	03-01-2007	5024	11	11-07-2009	18444
2	18-02-2007	5695	12	26-08-2009	19115
3	06-07-2007	7708	13	11-10-2009	19786
4	06-10-2007	9050	14	26-11-2009	20457
5	21-11-2007	9721	15	11-01-2010	21128
6	06-01-2008	10392	16	26-02-2010	21799
7	21-02-2008	11063	17	29-08-2010	24483
8	08-10-2008	14418	18	14-10-2010	25154
9	08-01-2009	15760	19	29-11-2010	25825
10	23-02-2009	16431	20	01-03-2011	27167

Table 3: ALOS track 365 data archive constitution.

	Acquisition date	Orbit number		Acquisition date	Orbit number
1	05-12-2006	4601	12	25-01-2009	16008
2	20-01-2007	5272	13	12-06-2009	18021
3	07-06-2007	7285	14	28-07-2009	18692
4	23-07-2007	7956	15	12-09-2009	19363
5	07-09-2007	8627	16	28-10-2009	20034
6	08-12-2007	9969	17	13-12-2009	20705
7	23-01-2008	10640	18	30-04-2010	22718
8	09-03-2008	11311	19	31-07-2010	24060
9	25-07-2008	13324	20	15-09-2010	24731
10	09-09-2008	13995	21	16-12-2010	26073
11	10-12-2008	15337	22	31-01-2011	26744

Table 4: ALOS track 366 data archive constitution.

	Acquisition date	Orbit number		Acquisition date	Orbit number
1	22-12-2006	4849	11	29-06-2009	18269
2	06-02-2007	5520	12	14-08-2009	18940
3	24-06-2007	7533	13	29-09-2009	19611
4	09-08-2007	8204	14	14-11-2009	20282
5	09-02-2008	10888	15	30-12-2009	20953
6	26-03-2008	11559	16	14-02-2010	21624
7	11-08-2008	13572	17	17-08-2010	24308
8	26-09-2008	14243	18	02-10-2010	24979
9	27-12-2008	15585	19	02-01-2011	26321
10	11-02-2009	16256	20	17-02-2011	26992

Table 5: ALOS track 367 data archive constitution.

	Acquisition date	Orbit number		Acquisition date	Orbit number
1	08-01-2007	5097	12	13-01-2009	15833
2	11-07-2007	7781	13	28-02-2009	16504
3	26-08-2007	8452	14	16-07-2009	18517
4	11-10-2007	9123	15	31-08-2009	19188
5	11-01-2008	10465	16	16-10-2009	19859
6	26-02-2008	11136	17	01-12-2009	20530
7	12-04-2008	11807	18	16-01-2010	21201
8	28-05-2008	12478	19	03-03-2010	21872
9	28-08-2008	13820	20	03-09-2010	24556
10	13-10-2008	14491	21	19-10-2010	25227
11	28-11-2008	15162			

Table 6: ALOS track 368 data archive constitution.

	Acquisition date	Orbit number		Acquisition date	Orbit number
1	25-01-2007	5345	8	17-09-2009	19436
2	12-06-2007	7358	9	02-11-2009	20107
3	28-07-2007	8029	10	18-12-2009	20778
4	13-12-2007	10042	11	02-02-2010	21449
5	14-09-2008	14068	12	05-08-2010	24133
6	30-01-2009	16081	13	05-11-2010	25475
7	02-08-2009	18765			

Table 7: ALOS track 369 data archive constitution.

	Acquisition date	Orbit number		Acquisition date	Orbit number
1	27-12-2006	4922	11	01-01-2009	15658
2	11-02-2007	5593	12	16-02-2009	16329
3	29-06-2007	7606	13	04-07-2009	18342
4	14-08-2007	8277	14	04-10-2009	19684
5	29-09-2007	8948	15	04-01-2010	21026
6	14-11-2007	9619	16	22-05-2010	23039
7	30-12-2007	10290	17	07-07-2010	23710
8	14-02-2008	10961	18	22-08-2010	24381
9	31-03-2008	11632	19	07-10-2010	25052
10	01-10-2008	14316	20	07-01-2011	26394

Table 8: ALOS track 370 data archive constitution.

Figure 5 shows the temporal distribution of the ALOS tracks 364, 365, 366, 367, 368, 369 and 370 data archive used in the study. As can be observed the sampling gives at least two images per year. It is important to remark that each acquisition represents a measurement in time.

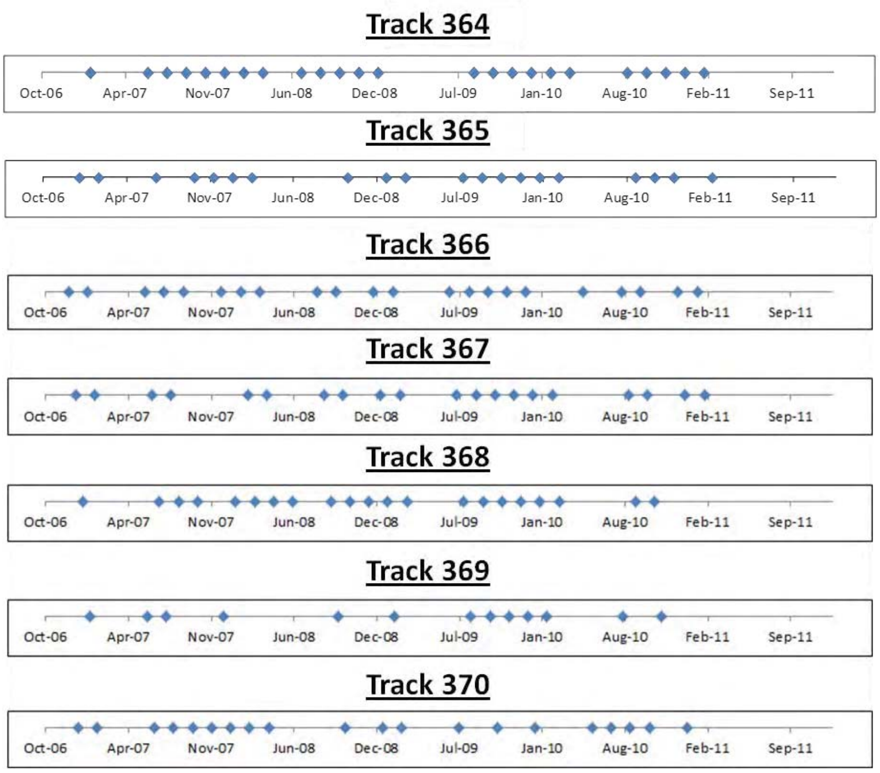

Figure 5: Time distribution of the images. Each acquisition date will represent a measurement.

5. TERRAIN MOTION DETECTION METHODOLOGY

5.1. SPN INTERFEROMETRIC PROCESS

The ALOS radar satellite data was processed using the Stable Point Network (SPN) interferometric software. SPN is an algorithm belonging to the Persistent Scatterer Interferometry (PSI) family of software. Developed by Altamira Information, SPN is able to utilise the SAR data acquired by the space-borne sensors (ALOS PALSAR-1 in this case) to extract precise displacement and position information of radar stable points.

PSI algorithms work by identifying high quality reflectance points in the radar imagery. Once identified model fitting methodologies are applied to these high quality points to derive the precise height and displacement measurements.

The algorithms are then applied to a set of input interferograms. Interferograms are images that represent the radar phase differences between a pair of SAR images. In an interferogram the phase value is related to the geometric configuration of the image pair, motion that has occurred during the period, atmospheric effects and noise.

The basis of the technique is the separation of the different components (deformation, topographic error and atmospheric effects) from the input data (see equation 1). Step-by-step, the data is processed taking into account the physical behaviour of each component characterised in terms of the radar signal reflectance and image geometry. Finally the atmospheric effects are estimated and eliminated as spatially low-wavelength and temporally high-frequency effects. Afterwards a high resolution analysis is carried out to extract the precise values of the deformation as well as the precise DEM correction values.

$$\Phi_{INTERF} = \Phi_{HEIGHT} + \Phi_{VEL} + \Phi_{APS} + \Phi_{NOISE} \quad [1]$$

The identification of measurement points can be based on the amplitude stability of the radar pixels or on the interferometric coherence of interferograms. In this case the medium resolution interferograms generated from the full resolution ALOS images have been used for the analysis. This procedure, called multi-looking, consists in the averaging of the response of several pixels (in this case 8x4) and has the effect of increasing the signal to noise ratio of the data at the expense of resolution. The processing resolution was of 35x35 meters. The final geocoding precision obtained using the DEM correction factors is approximately of 10m.

5.2. TRACK MERGING

The areas of interest of each client are covered with several overlapping tracks, as it was shown in Figure 4. These tracks of SAR images contain many frames (see Table 1). The partial overlap between tracks must be handled properly; the objective of this section is to illustrate how this was achieved.

It is important to bear in mind that the number of SAR images and the acquisition dates are specific for each track, since they are captured by different satellite passes and at different moments in time. Figure 5 shows the different measurements in time for every track. Due to the difference in date there are two SPN measurements in the overlapping areas. This data is used to calibrate the results between tracks, always using the best quality track as reference. The calibration values used are obtained from good quality common points in the calibration areas, see Figure 6. Therefore, a unique reference point is set in the central track 366 and a constant value is corrected from the nearby tracks.

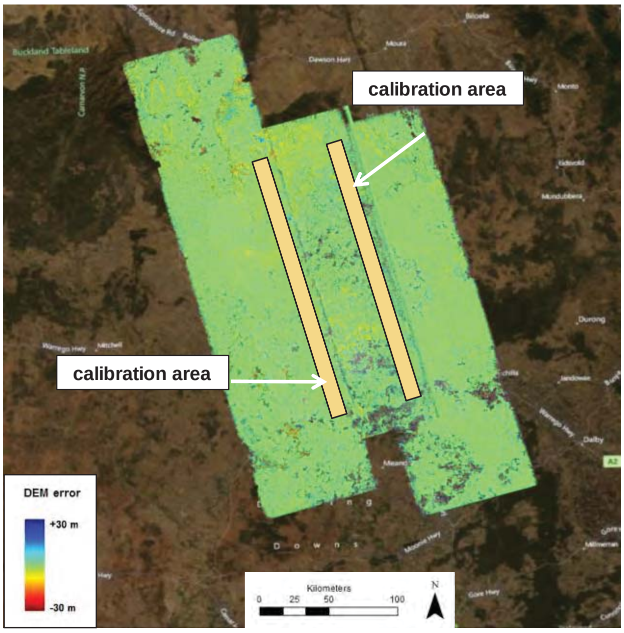

Figure 6 : Track merging and calibration areas between tracks

In the overlapping areas the information is not duplicated, only measurements of one track have been used for the final deliveries. Depending on the particular conditions of each location, the decision of which track was used was a function of the relative quality of the measurements.

Masks have been applied to delimitate the borders between tracks and define the sectors of the overlapping areas which are going to have measurements of either of the neighbouring tracks. The masking criteria used included the quality of the track, type of land cover and local topography, see Figure 7.

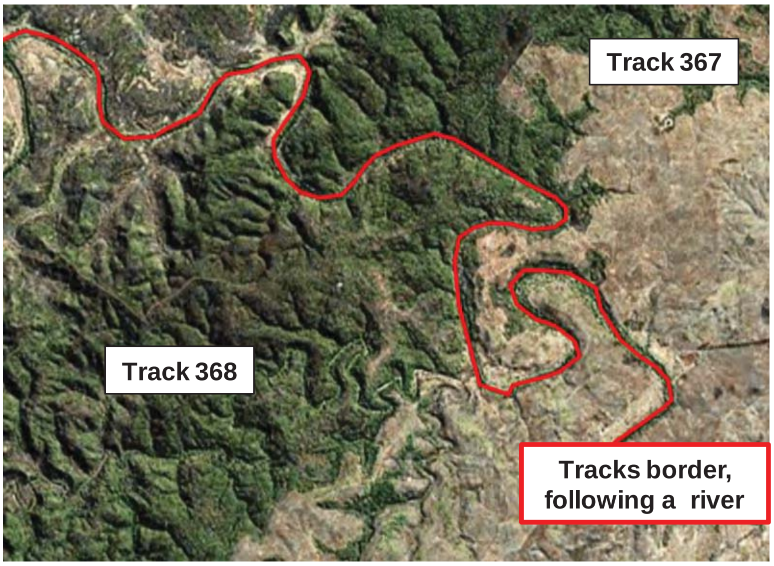

Figure 7 : Example of masking procedure between tracks

6. DELIVERED PRODUCTS

The delivered products have been produced separately for each client for their respective area of interest, without including data from other client areas. The product was divided in smaller areas and delivered in batches at different times. Each batch included vectors, geocoded images and map files.

6.1. VECTOR FILES

The vector files contain the database with the details of the ground motion through time for each measurement point (Time Series), including its location, absolute accumulative displacement (with respect to a spatial and temporal reference), the mean annual displacement rate and the main InSAR processing quality parameters. This database was delivered in an ESRI Shape file format (.shp). Due to the database size, the Shape file was divided into more than one vector file for computational efficiency, following a quadrants division layout structure.

6.2. DATA STRUCTURE

The database contains all the detailed information of the measurements. Each line of the database represents one measurement point containing its related data. Table 9 shows an example of the data given for two measuring points. The first seven columns provide information about the location of the measurement point, in ground and in SAR geometry. The next columns detail the main measurements (point vertical height and mean annual rate of deformation) and the main quality parameters. The last columns represent the time series of the points with the ground motion measured for each correspondent acquisition date. There are as many columns for time series as SAR acquisitions used in the processing. A detailed description of these parameters is given below.

CODE	LONGITUDE	LATITUDE	EASTING	NORTHING	RANGE	AZIMUTH	ERH	VEL	COH_STDDEV
T367_F664_F667_01708_04093	149.723892	-26.147972	772298.4	7105078.0	1708	4093	1.62	1.59	0.84
T367_F664_F667_01708_04094	149.723846	-26.147745	772293.0	7105103.5	1708	4094	1.02	1.29	0.88

COH_VEL	STDDEV_TS	MEAN_COH	STDDEV_ERH	STDDEV_SUB	PROJCODE	24/06/2007	09/08/2007	N acquisitions	17/02/2010
0.84	3.98	0.42	0.58	0.70	28355	-0.92	0.00	• • •	-3.47
0.86	3.81	0.43	0.49	0.60	28356	-5.73	-8.91		-21.14

Table 9 : Example of a vector file database parameters. Only three dates of the Time Series are shown in this example (the two initials and the last one).

The data fields are divided in four sets:

Position:

- CODE: Unique identifier label for each measurement point.
- LONGITUDE: Geographical Longitude position [decimal degrees over WGS84].
- LATITUDE: Geographical Latitude position [decimal degrees over WGS84].
- EASTING: UTM Easting in Geodetic Datum Australia 94 zone 55 [meters].
- NORTHING: UTM Northing in Geodetic Datum Australia 94 zone 55 [meters].
- RANGE: SAR geometry range (column) [image samples].

- AZIMUTH: SAR geometry azimuth (line) [image samples].
- PROJCODE: Code that defines the UTM zone

Measurement:

- ERH: Height error (correction factor) with respect to the DEM used for the interferogram generation [meters].
- VEL: Ground motion mean velocity value measured for the observation period [mm/year].

Quality:

- COH_VEL: Quality measure which relates to the SPN model (average annual displacement rate and DEM error) fit. Values between 0 and 1, where 1 indicates best fit. The fitting quality depends on the characteristics of each processing, like the number of images used, the noise level of the measurement point and the reliability of the model fitting. For a standard SPN processing, the values of quality for the estimation of the annual average displacement can be divided in the following categories:
    - 0,8 – 1,0 Very reliable
    - 0,5 – 0,8 Reliable
    - 0,2 – 0,5 Medium (might be a point that has a strong non-linear movement, or a not constant vertical height level or presenting significant noise levels)
    - 0,0 – 0,2 Low (Measurement errors, no such points delivered)
- STDDEV_TS: Standard deviation of the time series (TS) of the point with respect to a linear fit. Values closest to 0 indicate the least variation from a linear fit. In general a point with high coherence has a low dispersion. An exception to this rule might be a point that has seasonal movements or non-linear motion [mm].
- MEAN_COH: Average of interferometric coherence of all the interferograms used. This value is related to the interferometric phase stability of the point over the time. Values are between 0 and 1, 1 being the maximum quality. This parameter is useful to identify areas of good signal to noise ratio at the input data.
- COH_STDDEV: Standard deviation of the measured mean coherence (MEAN_COH). This parameter gives an indication of the variability of the phase stability over time. This parameter is useful to identify points affected by temporal changes as they do not give a constant coherence value over time.
- STDDEV_SUB: This parameter indicates the standard deviation of the ground motion mean velocity value measured for the observation period [mm/year]. It is a statistical measure that expresses a lower bound on the variance of estimators of the deterministic parameters.

- STDDEV_ERH: Standard deviation of the point height estimation [meters]. It is a statistical measure that expresses a lower bound on the variance of estimators of the deterministic parameters.

Time series (TS):

- DATE: (e.g. 15/06/2011) Total accumulated movement value [mm] for every date with respect to the reference point. This value is set to 0.0 in the second acquisition, as it is used as the temporal reference due to its lower noise level in all of the seven tracks. An example of a time series is shown in Figure 8.
  The deliveries have been made using seven different satellite tracks to cover the whole area of interest. Depending on the client's areas of interest, in their individual delivery, some tracks were used while others were not. The acquisition date of the images is specific for each track, see Figure 5. The measurements of the tracks used in every client have been merged to create a unified database. The total database has a unique set of dates which comprises the acquisition dates for tracks involved. Each measurement point will only have a TS value on the dates corresponding to its track, in the other dates there is a -9999 mask value, see Table 10. In each date where the track does not have acquisitions, -9999 mask values are used. The label of the point allows identifying the track to which it belongs.

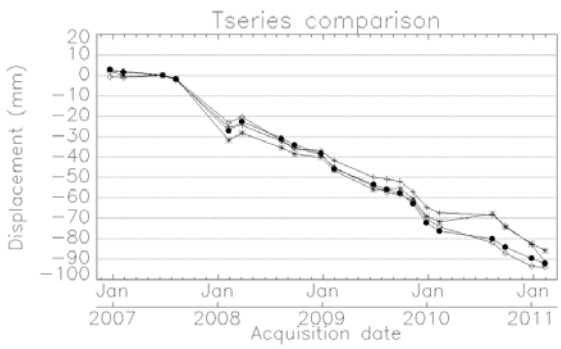

Figure 8: Time Series graph example showing the time evolution of the measured ground motion for this point.

	16/07/ 2009	28/07/ 2009	14/08/ 2009	31/08/ 2009	12/09/ 2009	29/09/ 2009	16/10/ 2009	28/10/ 2009	14/11/ 2009	01/12/ 2009	13/12/ 2009	30/12/ 2009
T366	-9999	-6.86	-9999	-9999	-6.81	-9999	-9999	-8.01	-9999	-9999	-7.69	-9999
T367	-9999	-9999	-3.67	-9999	-9999	-3.64	-9999	-9999	-2.44	-9999	-9999	-2.29
T368	1.37	-9999	-9999	0.73	-9999	-9999	0.89	-9999	-9999	1.29	-9999	-9999

Table 10: Example of twelve values for one point of each track in mm. In each date where the track does not have acquisitions, -9999 mask values are used.

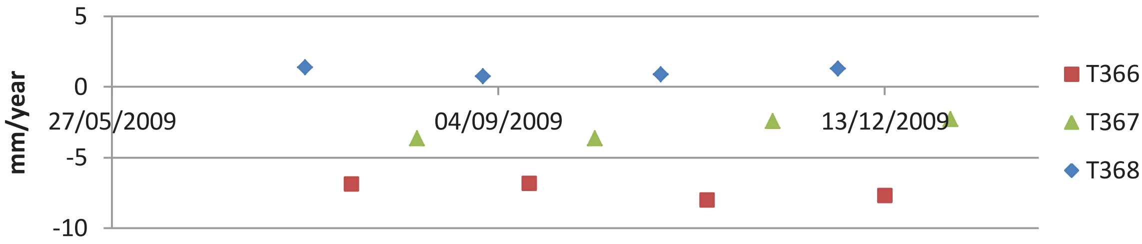

Figure 9: Time series of Table 2 data. Different tracks have different dates of acquisition. -9999 mask values have not been represented.

6.3. GEOCODED IMAGE FILES

This digital image contains the mean annual rate of ground motion retrieved from the SPN analysis. This file provides a rapid means of understanding the location and magnitude of any terrain-motions. Examination of the image will direct the course of any subsequent analysis. The magnitude of the motion of each point is specified using the colour scale showed in Figure 11.

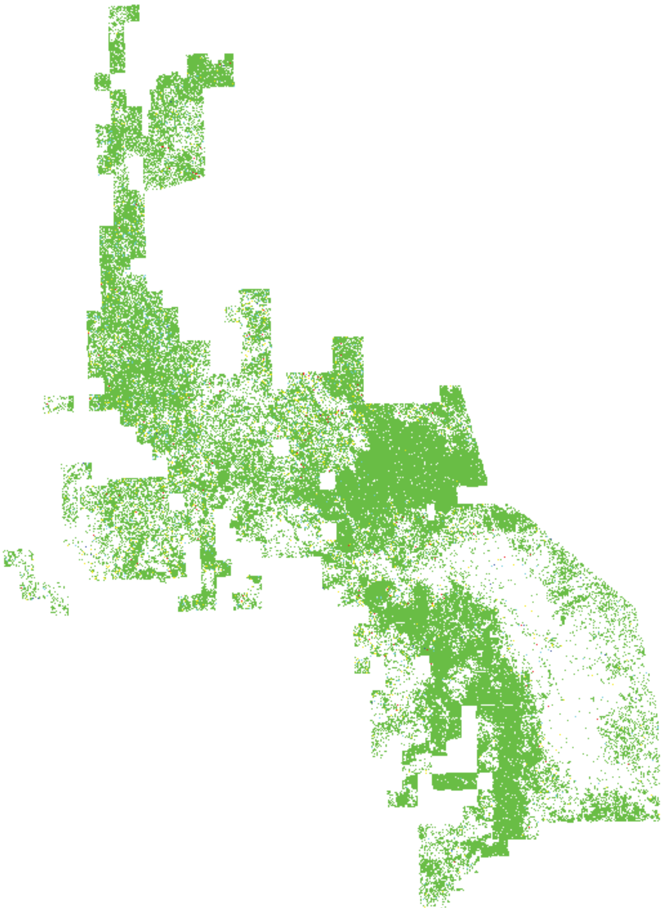

Figure 10: Geocoded image with the mean annual rate of deformation. The image has a white background (no measurements) which can be set as a transparent colour.

The georeference system used is Geodetic Datum Australia 94 UTM Zone 55 and Zone 56. The image can be displayed over a background reference image to understand the context of any motions.

The colour scale used for terrain-motion magnitude interpretation is shown in Figure 11.

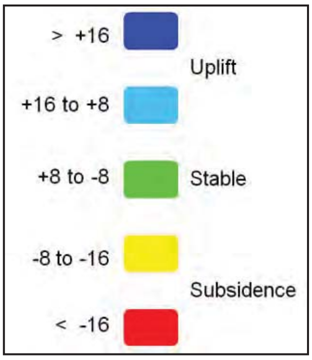

Figure 11: Mean annual displacement rate colour scale, in mm/year. The interval of stability is set from -8.0 to +8.0 mm/year.

6.4. MAP FILES

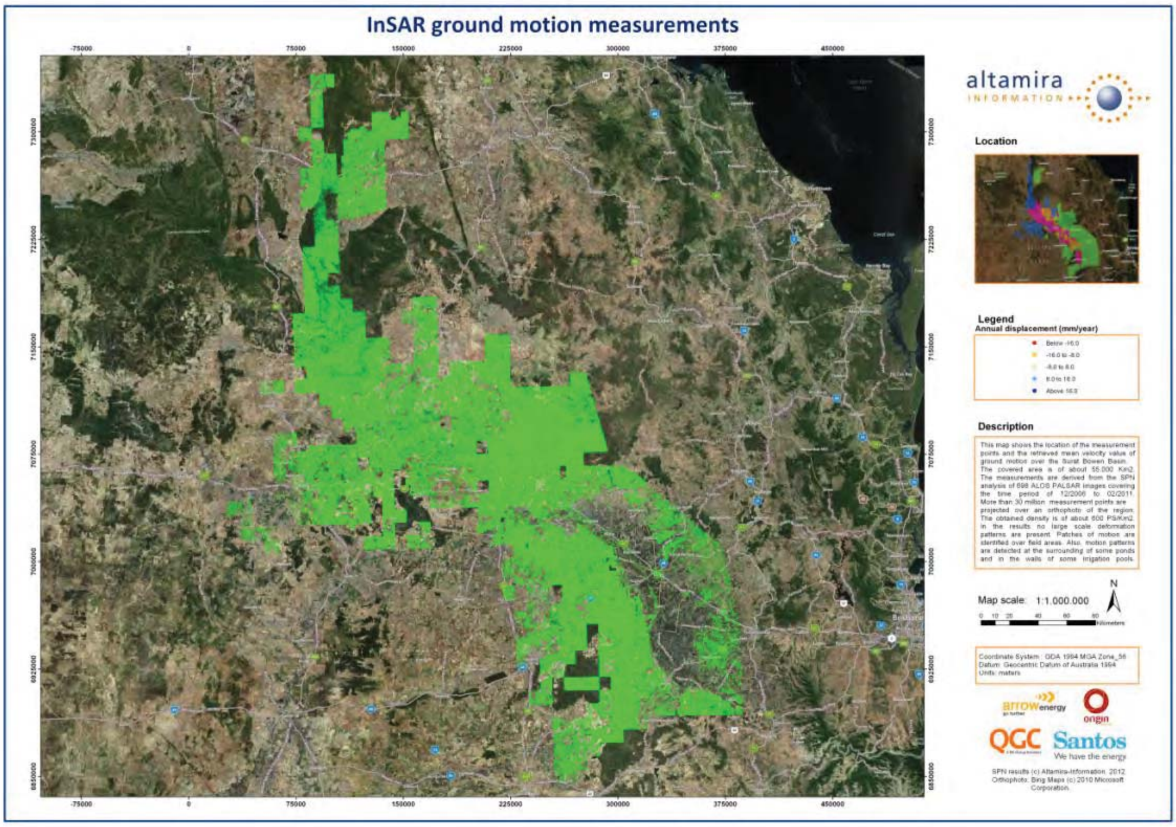

Figure 12: Example of a mean velocity map.

The map files contain the mean annual motion rate retrieved from the SPN analysis projected over a background image. A Bing Maps 2010 Microsoft Corporation © orthoimage has been used as background. Maps include: motion magnitudes colour legend, spatial legend, brief description and north direction indicator.

Maps were given to every client on each delivery using different scales in order to fit their needs. Due to the considerable extent of the areas, divisions were made and a map for each one was generated. The format of the map, both in physical and digital format, was DIN A2 (42 x 59.4 cm).

7. RESULTS OF THE BASELINE STUDY

This section presents the main results of the historical study concerning the measurement of ground surface motions. The monitoring period covers over four years, from December 2006 to February 2011. The full analysis has been conducted using Stable Point Network methodology applied to coherent points, using 698 ALOS SAR images from seven different tracks.

Results are presented as average annual deformation maps along with time series data for the period of study. They allow assessing any ground movement patterns that might be present over the processed area.

In this study, no significant large-scale ground deformations have been detected. However, several areas with local patterns of deformation were found that were related to natural or anthropogenic factors. Movement detected generally over irrigation pools and ponds, rural roads, fields and riverbanks.

It should be noted that this ground motion baseline assessment has been conducted over a period where the CSG extraction phase for each of the four proponents has yet to begin in full. As such any ground motion recorded is unlikely to be related to CSG extraction activities. However, there are several existing operational CSG fields in the study area where no significant ground surface motion has been detected by this study.

The ground motion data collection and processing methodology does not differentiate between natural processes, anthropogenic activities or CSG operations. Natural or anthropogenic effects on ground motion may include:

- Flooding: water covered areas does not reflect radar signals thereby “masking” flood extents
- 'Wetting and drying' effects (shrink and swell) of soils due to seasonal moisture variability
- Vegetation growth or removal
- Erosion, particularly on poorly vegetated hill slopes, and subsequent valley floor sedimentation (uplift)
- Natural long-term basin-wide compaction in both shallow and deeper formations

- Anthropogenic activities: the effects of ploughing fields, cropping, grazing and infrastructure development
- Existing groundwater use (e.g. irrigation, town supply, mining)

Some examples of where the results of this study include some of the above listed effects are provided in Appendix A. Additionally, the potential impact of strong rainfall on surface features is discussed further in Appendix B, as heavy rain events have been occurring during the period of analysis.

Some of these factors listed above may also impact the quality and the final density of the measurements. One important condition which should be met to perform the motion measurements is that the ground surface should remain invariant over time. All the elements over the ground surface should remain in the same way in order to achieve the same level of SAR signal over the repeat passes. Some of these factors originate then important superficial variations over the ground surface which reduces the quality of the SAR image over these areas and over time (temporal coherence). Important changes can originate significant drops of the temporal coherence resulting in the retrieval of few and valid data points of measurements. For example, agricultural fields that are ploughed regularly present generally a very low density of measurement points.

A brief study looking at the density and distribution of monitoring points and the relationship with surface coverage is presented in Appendix C. This study illustrates how the natural effects and the human activities that modify the landcover make difficult to obtain valid measurements over the affected areas, resulting in a notable decrease in the PS density because the SAR signal characteristics do not remain constant for the whole time period.

Figure 13 shows the average annual displacement rate of ground motion retrieved for the complete area of interest for all four proponents (Arrow Energy Pty, Australia Pacific LNG Pty (Origin), QGC Pty and Santos Limited). As can be seen, no large deformation patterns are visible and the region appears to be stable in general.

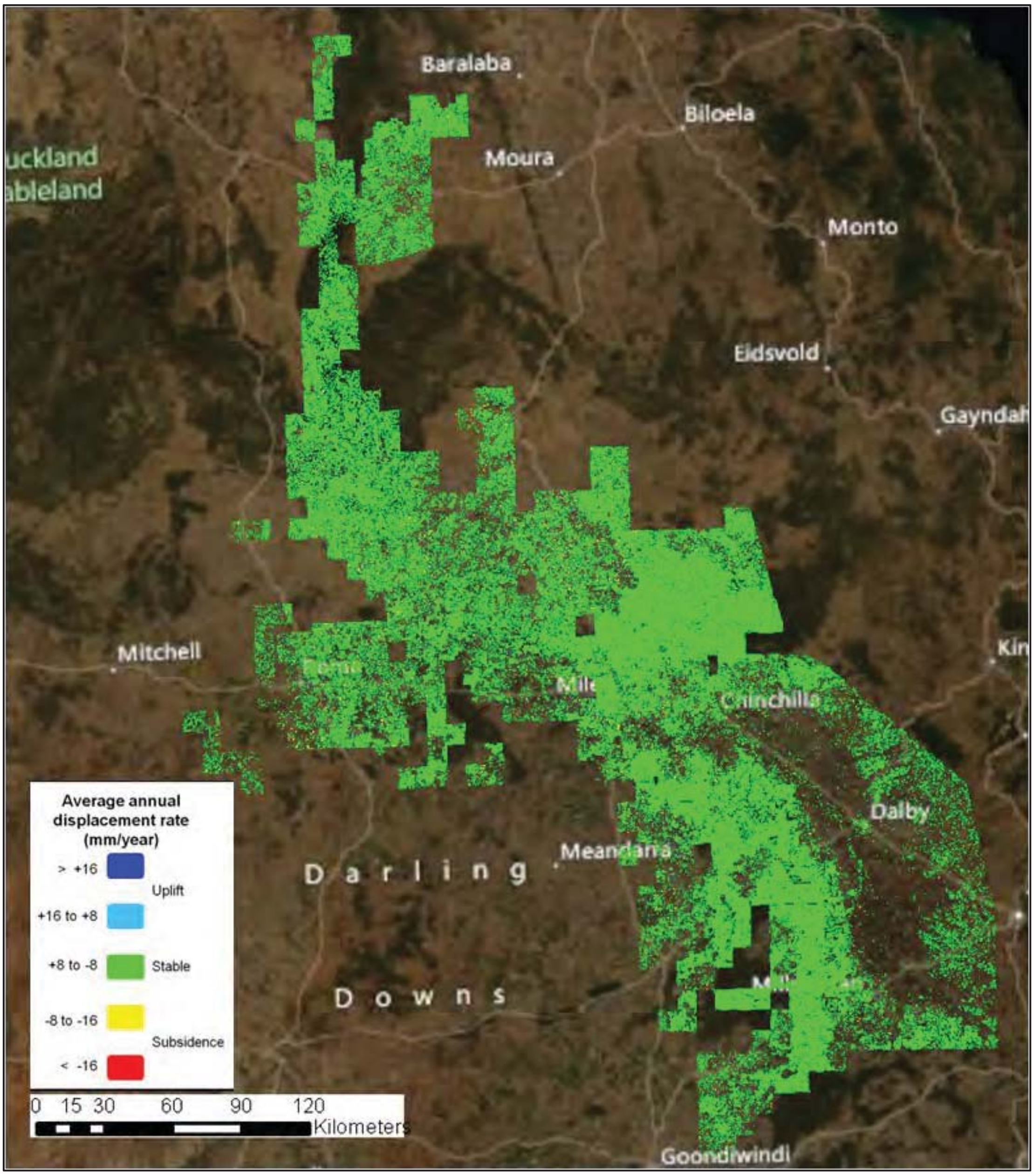

Figure 13: Average annual displacement rate map for the study areas.

Figure 13 shows also that the majority of the measurement points present stability (green colour, which means a motion below ±8 mm/year). Figure 14 presents the result of a numerical analysis of the global motion detected over the area. The histogram shows that a 97% of the total present stability. Only 0.3% of the points have a magnitude of ground motion higher than 15mm/year. The location of these points with motion is distributed through the area of interest and do not follow any significant large-scale spatial trend.

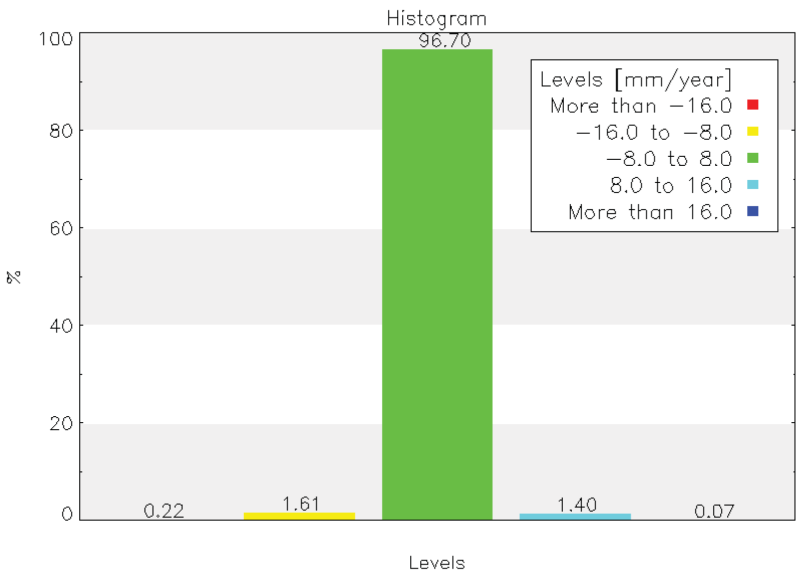

Total number of points	density
Over 30 million	600 PS/Km²

Figure 14 : Histogram showing percentage of the measurement points in each interval

Therefore, the main important conclusion that can be stated from the analysis is that there is no large-scale motion affecting the area of interest for the considered period. However, many small isolated zones with moderate ground motion patterns can be identified. Some of these areas identified have had a more detailed analysis completed, with the findings presented Appendix A.

8. CONCLUSIONS

The baseline study discussed in this report has demonstrated that InSAR data well suited for large areal-scale detection and monitoring of ground motion in areas like the Surat Basin. The area of interest is a very large (55.000 Km^2) rural area composed by fields, vegetated areas and crops with occasional manmade structures. Despite of the nature of the area, a large number of measurements (about 600 PSs/Km^2) were available to assess the magnitude and scale of ground motion for a four year period prior to the commencement of intensive CSG development.

The total number of measurement points obtained for the entire baseline program was over 30 million points for the area of interest. The PSI analysis of the whole area required the processing of a stack of 698 ALOS SAR images for the period December 2006 to February 2011.

The results of this study do not show any large scale pattern of ground motion, with the majority of the study area exhibiting stable conditions (less than 8mm of ground motion per year of the study).

The InSAR analysis has shown areas of natural/anthropogenic ground deformation in space and time and independent of CSG extraction activities. These areas are heterogeneously distributed within the study area. Examples of areas of subsidence include: fields, rural tracks, and the walls of some irrigation storages. Additionally, several uplift patterns are observed along selected riverbanks, possibly related with the heavy rains that occurred during 2010.

The completion of this project has resulted in the development of a regional baseline dataset for ground motion prior to large scale Coal Seam Gas extraction operations commencing across the Surat and Bowen Basins. The establishment of regional ground motion baseline allows for comparisons with future ground motion monitoring data to assess the effects of CSG production on surface subsidence.

9. MOVING FORWARD

For future InSAR monitoring of the Surat Bowen Basin, ALTAMIRA INFORMATION intends to use the data provided by the Radarsat-2 satellite. This satellite was launched in December 2007 by the Canadian Space Agency (CSA) and has a nominal life expectancy of 10 years (although twice of that service length is expected), and presents important technical advancements with respect to former C-band missions (Radarsat-1 or ERS/ENVISAT). ALTAMIRA INFORMATION has a long experience in the handling and processing of data images from the Radarsat-2 satellite with very successful results in rural and urban environments, so the transition to this new satellite should not present any new challenges.

The selection of this new satellite was based on several parameters:

- Type of land cover: X-band or C-band sensors perform in a different way depending on the land cover. X-band gives more density of points over infrastructure while C-band sensors give a more uniform distribution between vegetated areas and infrastructures. Altamira has many years of experience using both types of band in different scenarios and considering the land cover on the Surat Bowen Basin, C Band will provide a larger density of natural reflectors for long term monitoring periods.

- Extension of the AOI that must be covered: The ground coverage given by the images offered by each of the sensors must be considered, especially when the area of interest is so large and data is high resolution. In that case wide swath acquisition modes are preferred in order to reduce the number of required frames. Radarsat-2 offers very interesting wide swath acquisition modes while keeping the image resolution.

- Frequency of the deliverables: the required frequency of update of the measurements is another significant issue. InSAR measurements are possible each time there is an acquisition (although to perform the initial set-up network of natural reflectors for the measurements a minimum stack of images is required). However, depending on the project needs the delivery of the measurements can be performed at different frequencies (several times per year up to once per year). The maximum capacity of revisit time varies from one image each 8 days up to one image per month. As the new missions can be programmed the frequency of acquisitions can be adjusted in function of the project needs. Nowadays Radarsat-2 provides a revisiting time of 24 days, which is good for the project requirements.

- SAR data continuity: in long term monitoring projects the availability of SAR data in the future and the connection with the current data stack is a very important matter. Several C-band SAR missions are going to be performed before the end of the mission life of Radarsat-2. ALTAMIRA INFORMATION has a proven experience in the combination of SAR data acquired by different sensors for ensuring the continuity of ground motion measurements (ERS & ENVISAT and TerraSAR-X and Cosmo-Skymed data).

As such the RADARSAT-2 system has been selected as the optimum solution considering the results of the study performed. This satellite will provide high resolution images with an appropriate revisit frequency covering the required needs of the monitoring as well as optimum wave penetration offered by the C-band wavelength. Finally, it will secure the long term availability of SAR data due to the future Radarsat constellation commissioning (planned for 2014) or can also link in with the Sentinel-1 C-band satellite future ESA Earth Observation mission (planned for 2013).

APPENDIX A: EXAMPLES OF AREAS WITH MOTION

In order to provide some examples, this section presents some areas with motion that were identified in the area of interest. Figure 15 to Figure 33 present a detailed view of each of these areas with a zoomed map and their respective time series, allowing the assessment of the spatial extent and the time evolution of the detected ground motion. A zoomed map of the possible vulnerable area is presented systematically in the lower right corner of the figures showing only the measurement points with motion in order to facilitate the interpretation of the motion pattern considering the land cover.

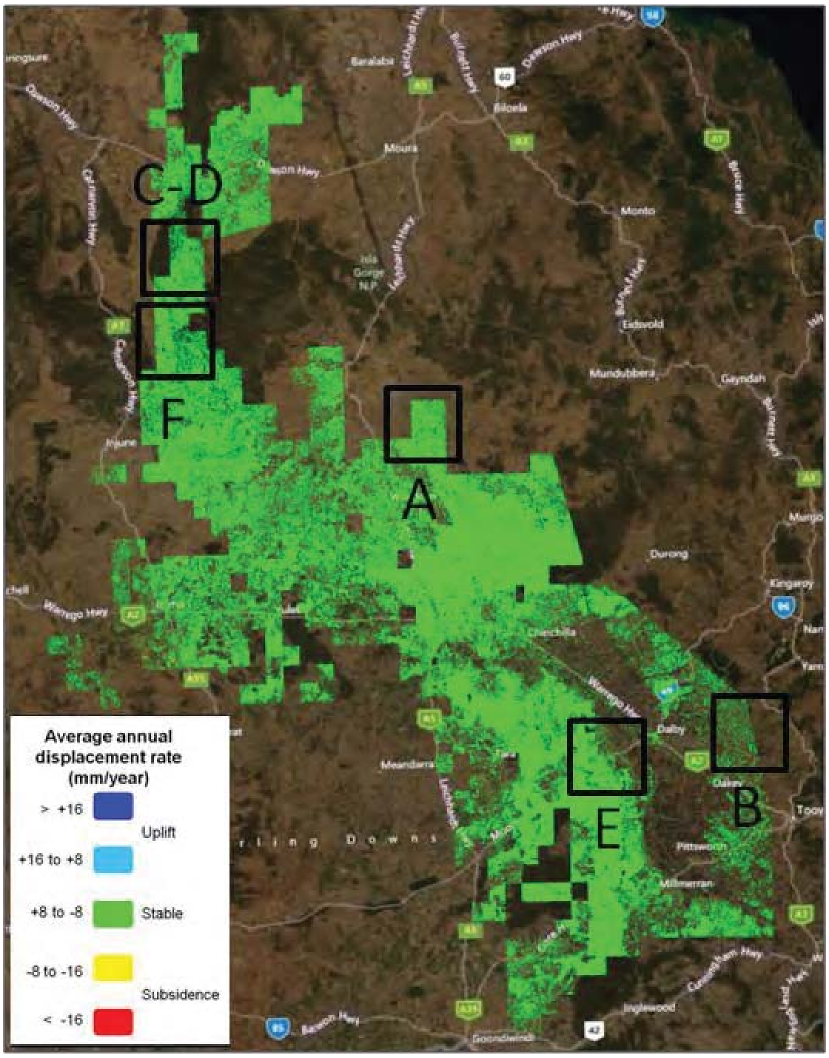

Figure 15: Identification of the example areas with motion based on the analysis of the mean annual displacement rate maps for the areas of interest.

A.1 AREA A

Figure 16 illustrates deformation areas A.1 and A.2. A.1 presents a very localised deformation pattern at the boundaries of a pond. All the time series, illustrated in Figure 17, show a similar trend of motion between 8.5 and 9cm for this area.

Area A.2 shows an uplift pattern detected along a riverbank. The time series over this area show an increase of the accumulated uplift during 2010 (Figure 18). This uplift might be the consequence of an increase of rainfall values over the area, known to have happened in 2010. Appendix B presents an example of correlation analysis of this type of ground motion with rainfall data and flooded areas.

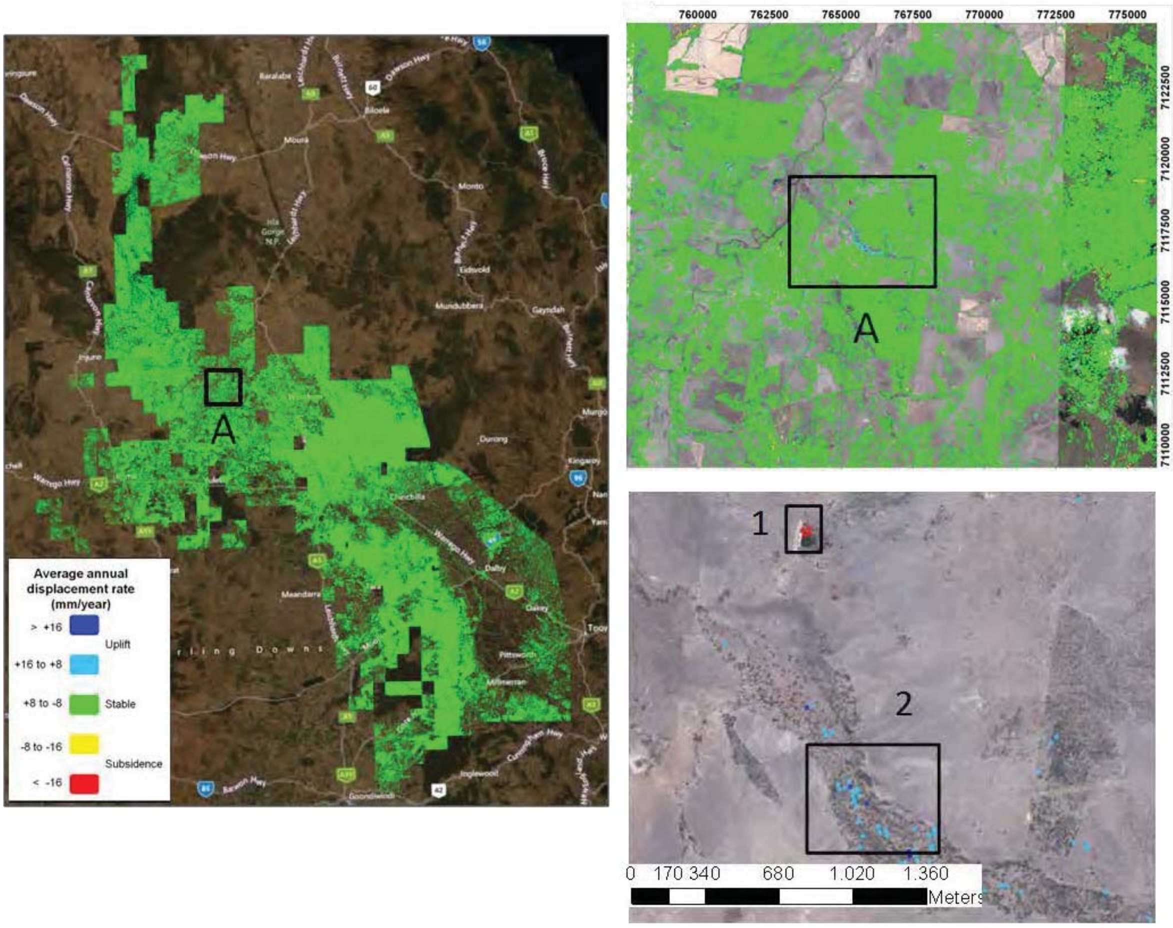

Figure 16 : Location and spatial extent of motion area A affected by ground motion

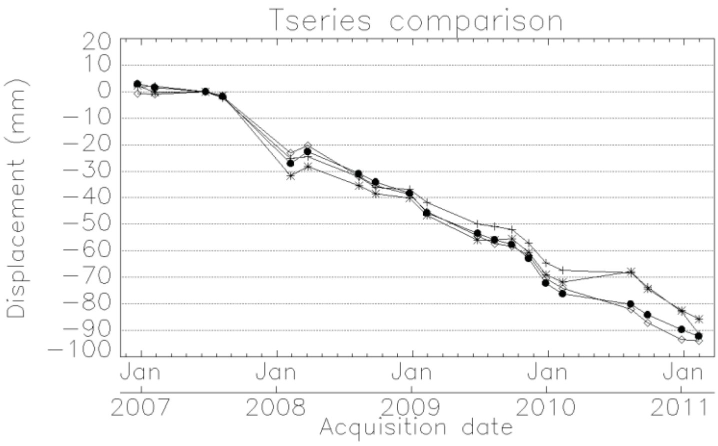

Figure 17 : Detailed time series of area A.1

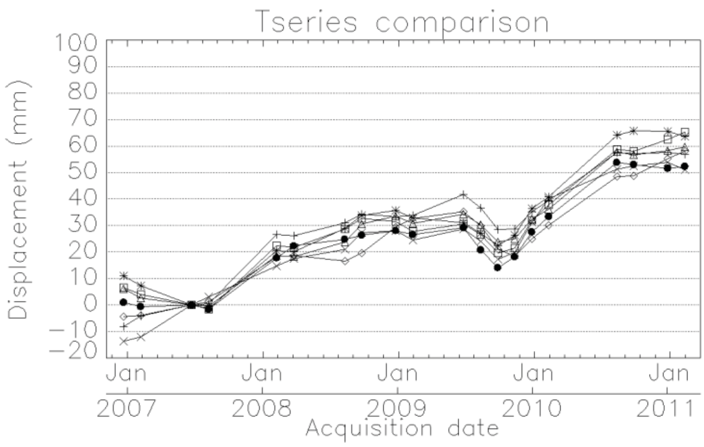

Figure 18 : Detailed time series of area A.2

A.2 AREA B

Figure 19 shows a deformation pattern over area B. A subsidence motion is detected over an area identified as the New Acland coal mine. Since it is an open cut mine that uses excavators and front-end loaders there are constant surface changes within the mine's boundaries. The ground surface is under continuous change which results in a decrease in the coherence of the measurements over the area.

However, several measurement points have been validated over the areas of the mine demonstrating ground motion patterns. In particular, Figure 19 presents a subsidence pattern, with a non-linear evolution in the time series (Figure 20), reaching an accumulated value of up to 8cm. As can be observed, the different time series follow the same trend of deformation with different magnitudes. This could imply that they are part of the same deformation system. The area marked "1" in Figure 19 below appears to show deformation around a haul road within the mine precinct.

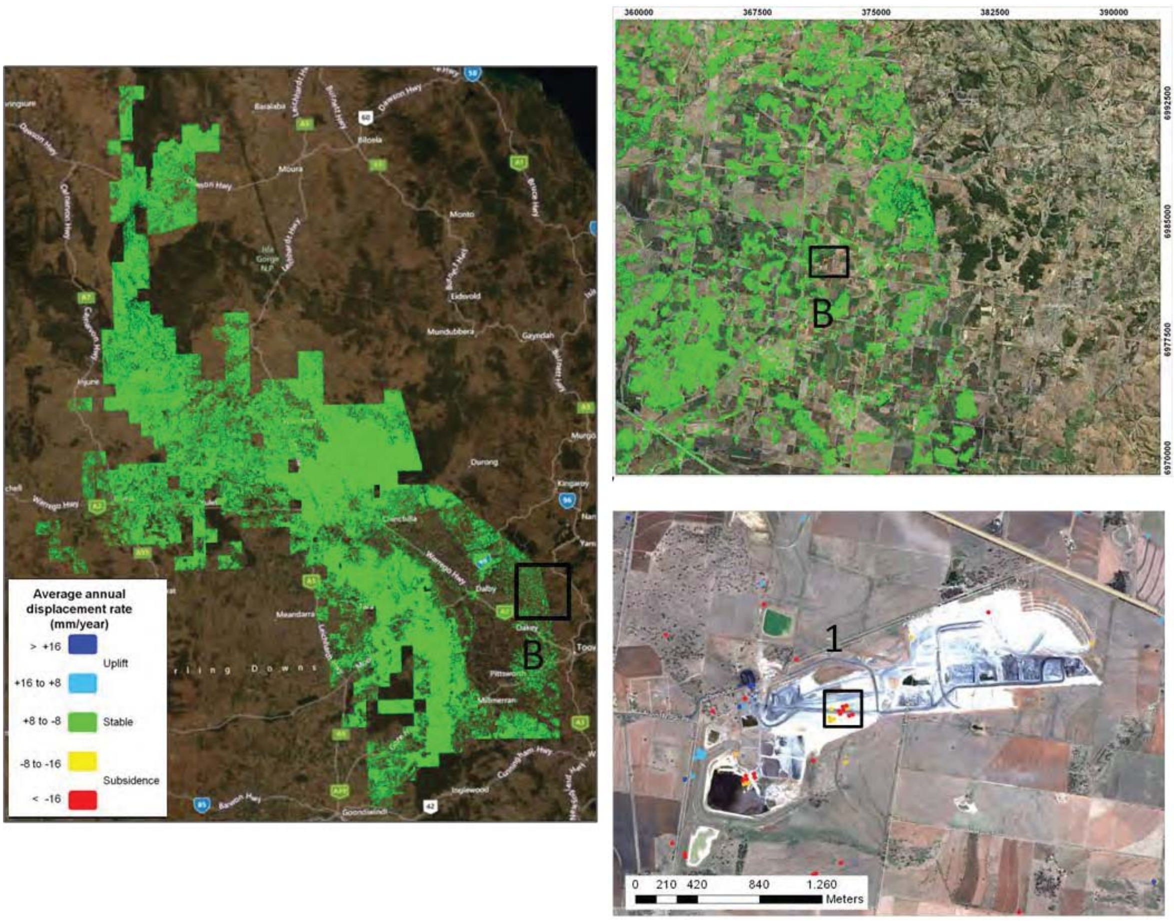

Figure 19 : Location and spatial extent of motion area B affected by ground motion

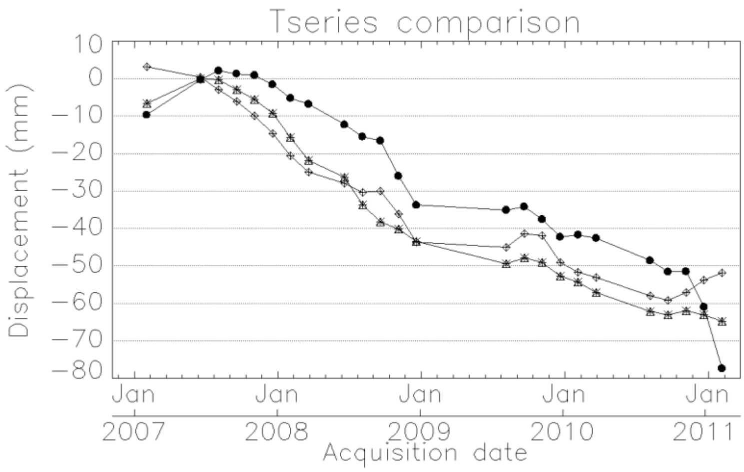

Figure 20 : Detailed time series of area B

A.3 AREA C

Figure 21 presents a subsidence pattern located over area C. Accumulated displacement of the time series in area C is up to 10cm (Figure 22). The deformation shown is located around an irrigation pool or pond. The time series have a non-linear behaviour and follow the same trend of deformation. The measured ground motion shows steady acceleration along the period of study, although some small variations can be seen.

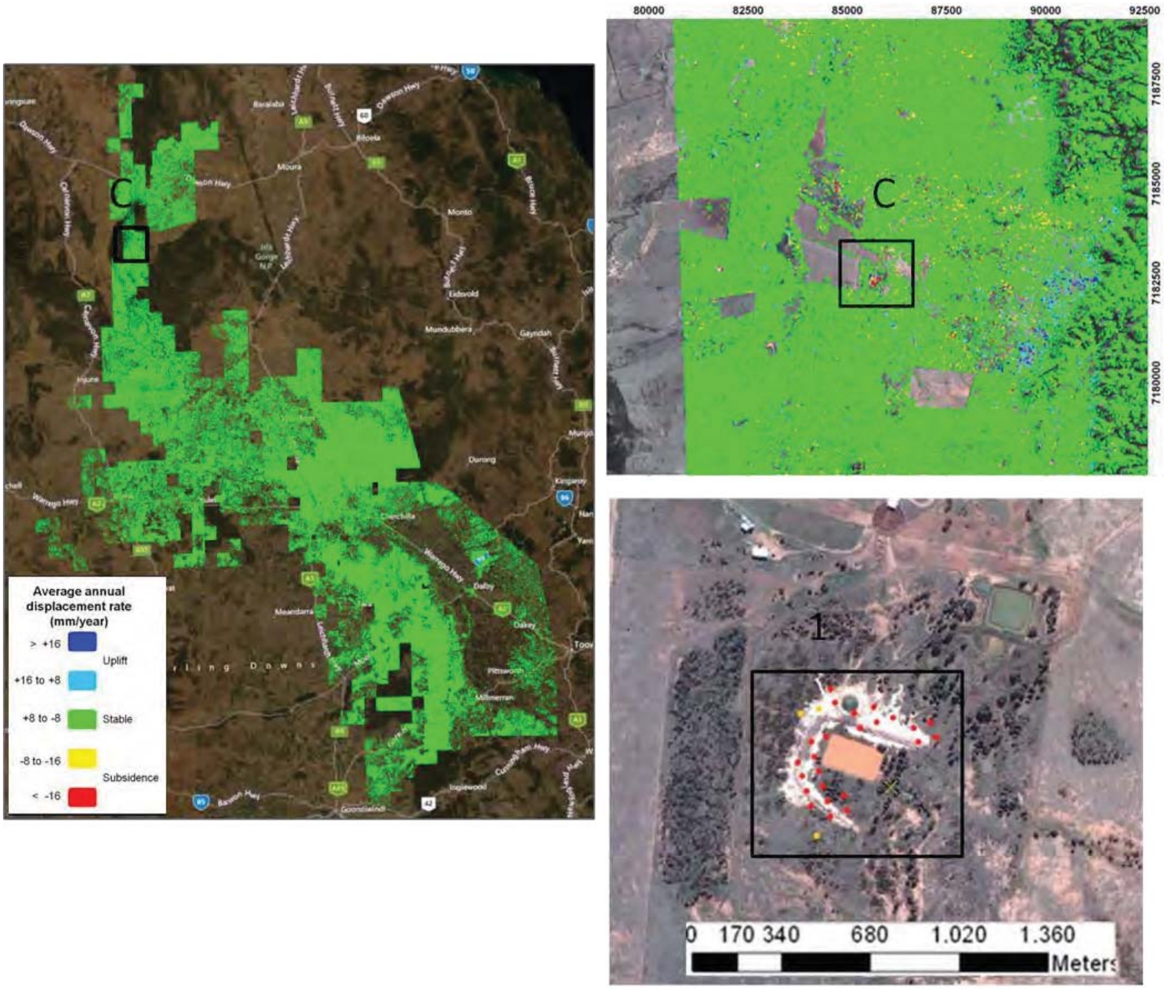

Figure 21: Location and spatial extent of motion area C affected by ground motion

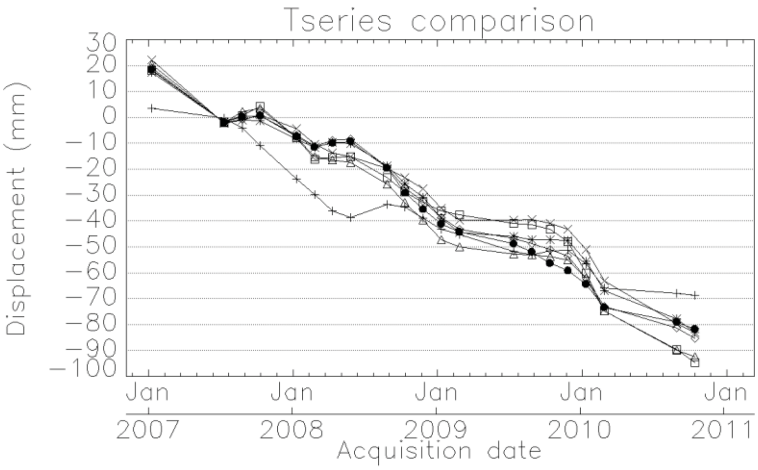

Figure 22 : Detailed time series of area C

A.4 AREA D

Figure 23 presents a subsidence pattern located over area D. Accumulated displacement of the time series is up to 15cm (Figure 24). The deformation shown is located over a mountainous area close to a rural road. The time series have a non-linear behaviour and follow the same trend of deformation. The acceleration can be considered as constant during the period of study. However, an exception during the year 2009 can be seen, where a period of stabilisation appears to have occurred.

Figure 25 shows a possible interpretation of the detected movement. The zone is presented in a 3-D view with the direction of the maximum gradient of the topography in the area of motion. The subsiding area is located in a steep slope below the mentioned rural road and probably follows a trend of deformation in the downhill direction.

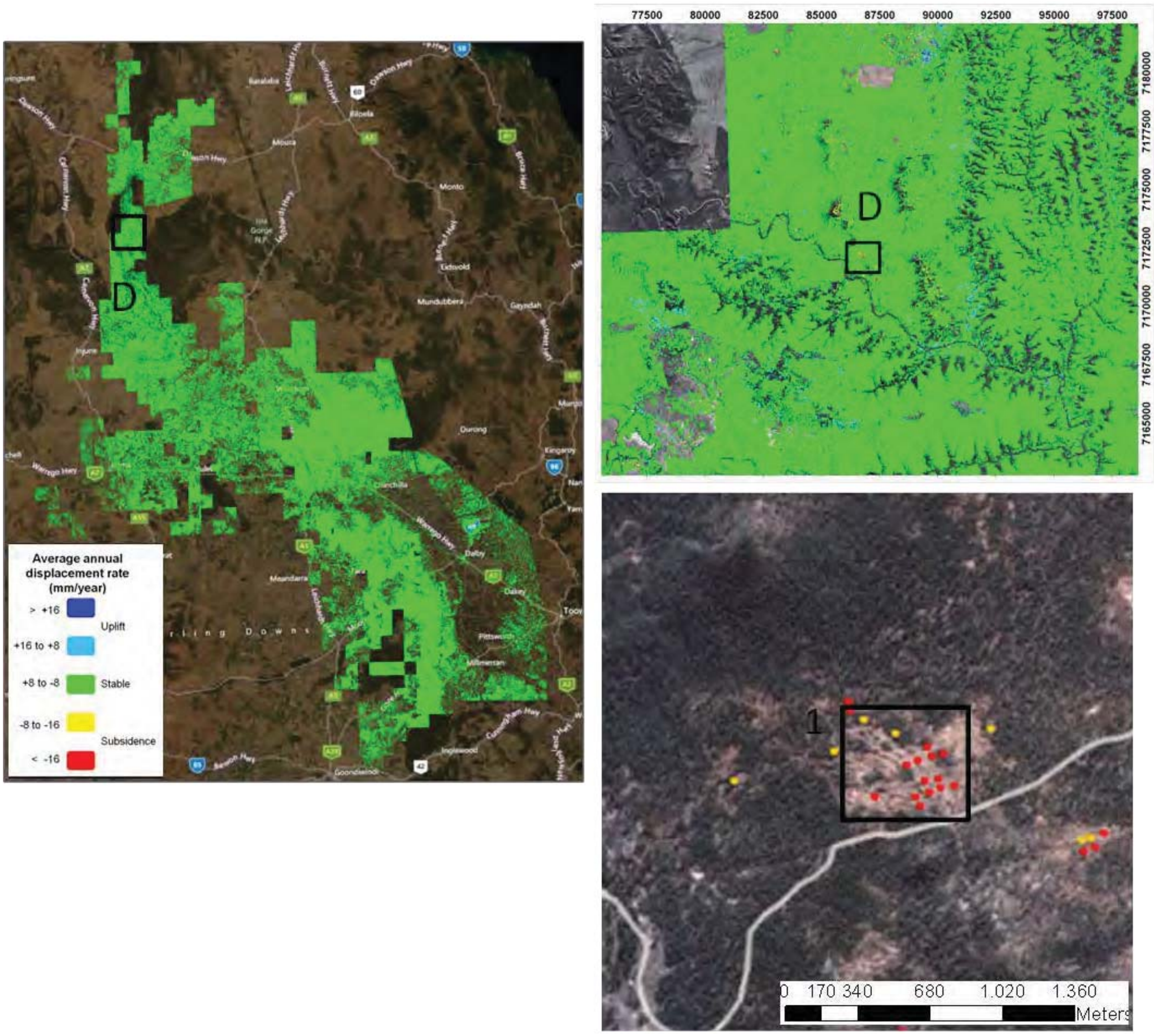

Figure 23 : Location and spatial extent of motion area D affected by ground motion

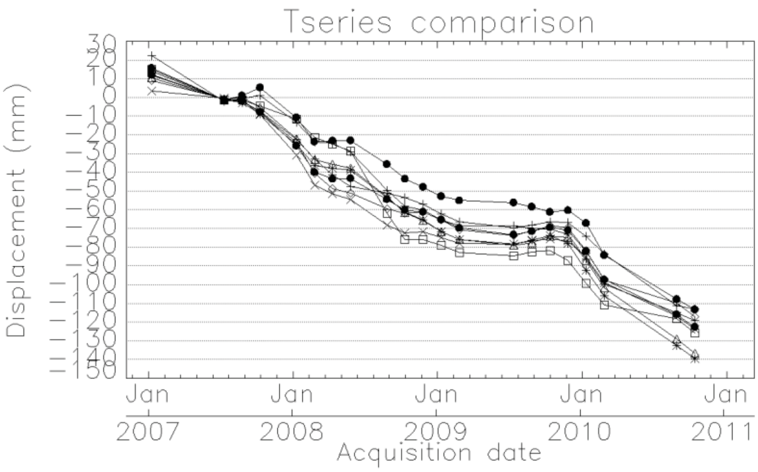

Figure 24 : Detailed time series of area D

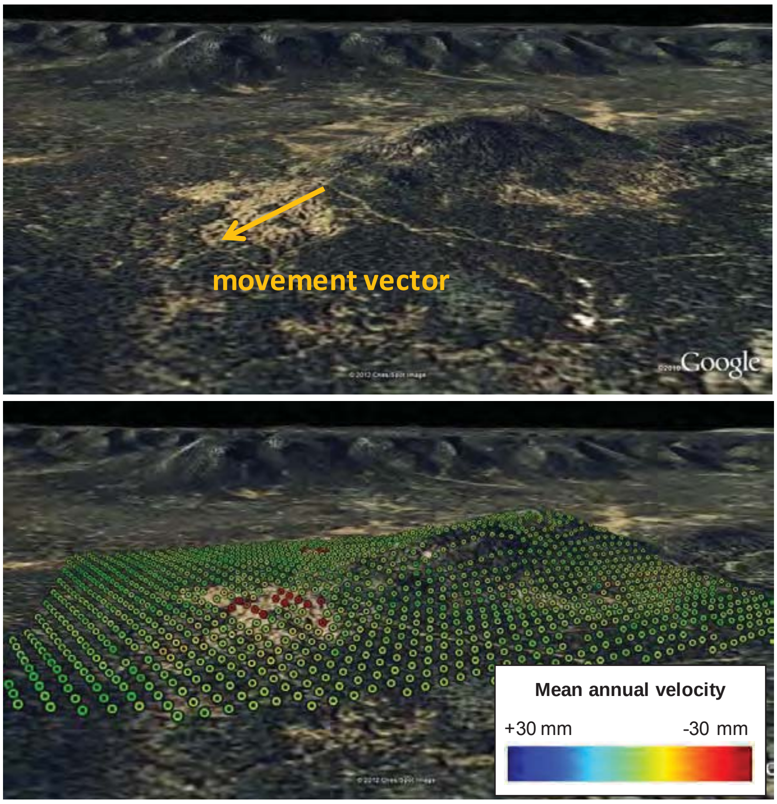

Figure 25 : Top image illustrates the topography of the area of interest and the movement vector of the detected subsidence. Bottom image shows the projected measurement points of area D.

A.5 AREA E

Figure 26, presents subsidence patterns located over area E. The time series in areas E.1, E.2 and E.3 (Figure 27, Figure 28 and Figure 29) present a similar time evolution of the displacement along the linear features in this area. This could indicate that these detected points with motion are part of the same deformation system. Accumulated displacement in area E.1 is of 15cm. In the case of E.2 and E.3 the accumulated value is of 9cm and 17cm respectively.

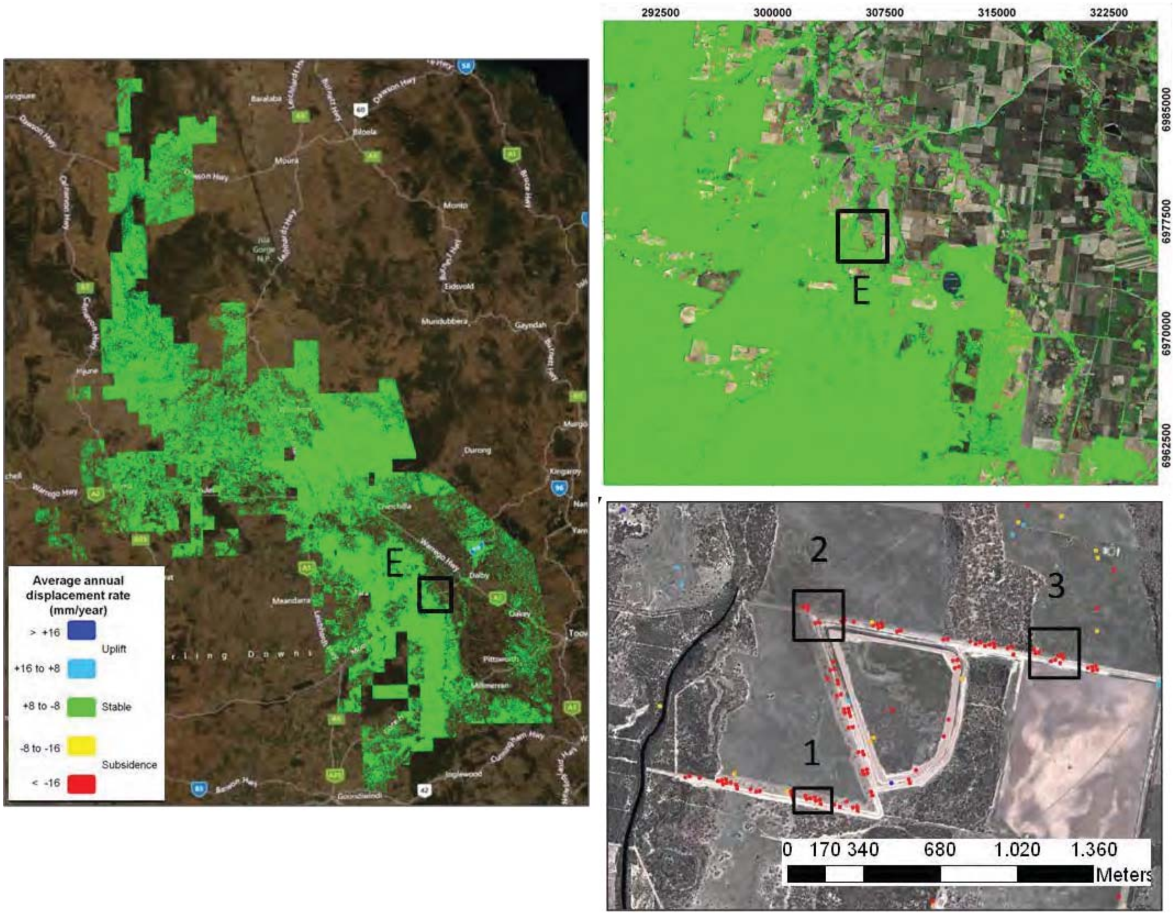

Figure 26 : Location and spatial extent of motion area E affected by ground motion

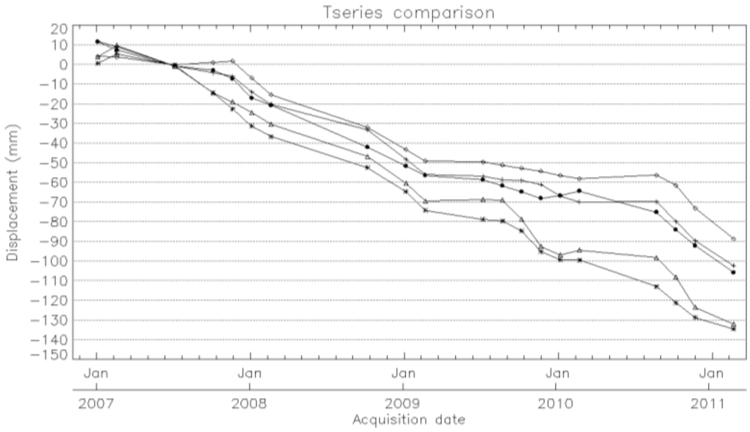

Figure 27 : Detailed time series of area E.1

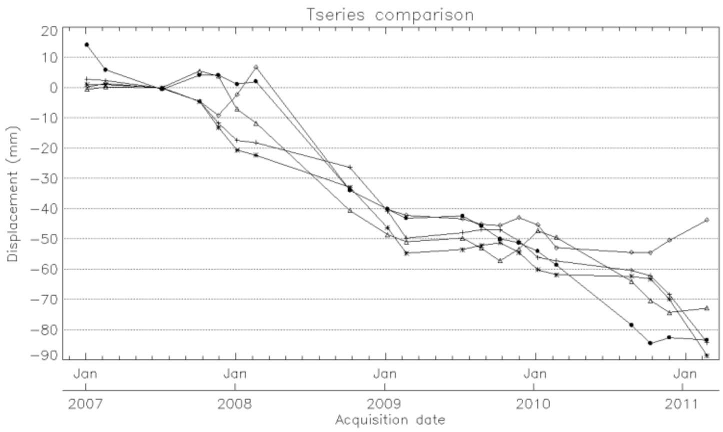

Figure 28 : Detailed time series of area E.2

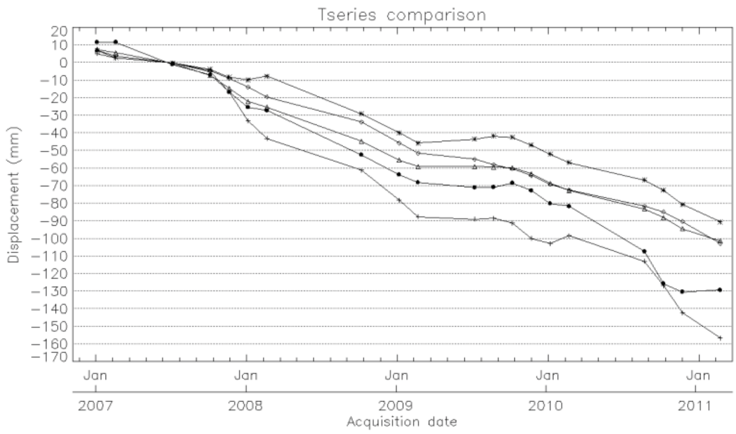

Figure 29 : Detailed time series of area E.3

A.6 AREA F

Figure 30 shows subsidence areas F.1, F.2 and F.3. Areas F.1 and F.2 present a subsidence pattern located around a pond or irrigation pool. Accumulated displacement of the time series is up to 6cm (Figure 31) and 8cm (Figure 32) respectively. The time series have a non-linear behavior and present a stabilization period during the year 2009. Area F.3 shows a subsidence pattern next to a rural road with a strong deformation magnitude. Accumulated displacement in this case is of 12cm (Figure 33).

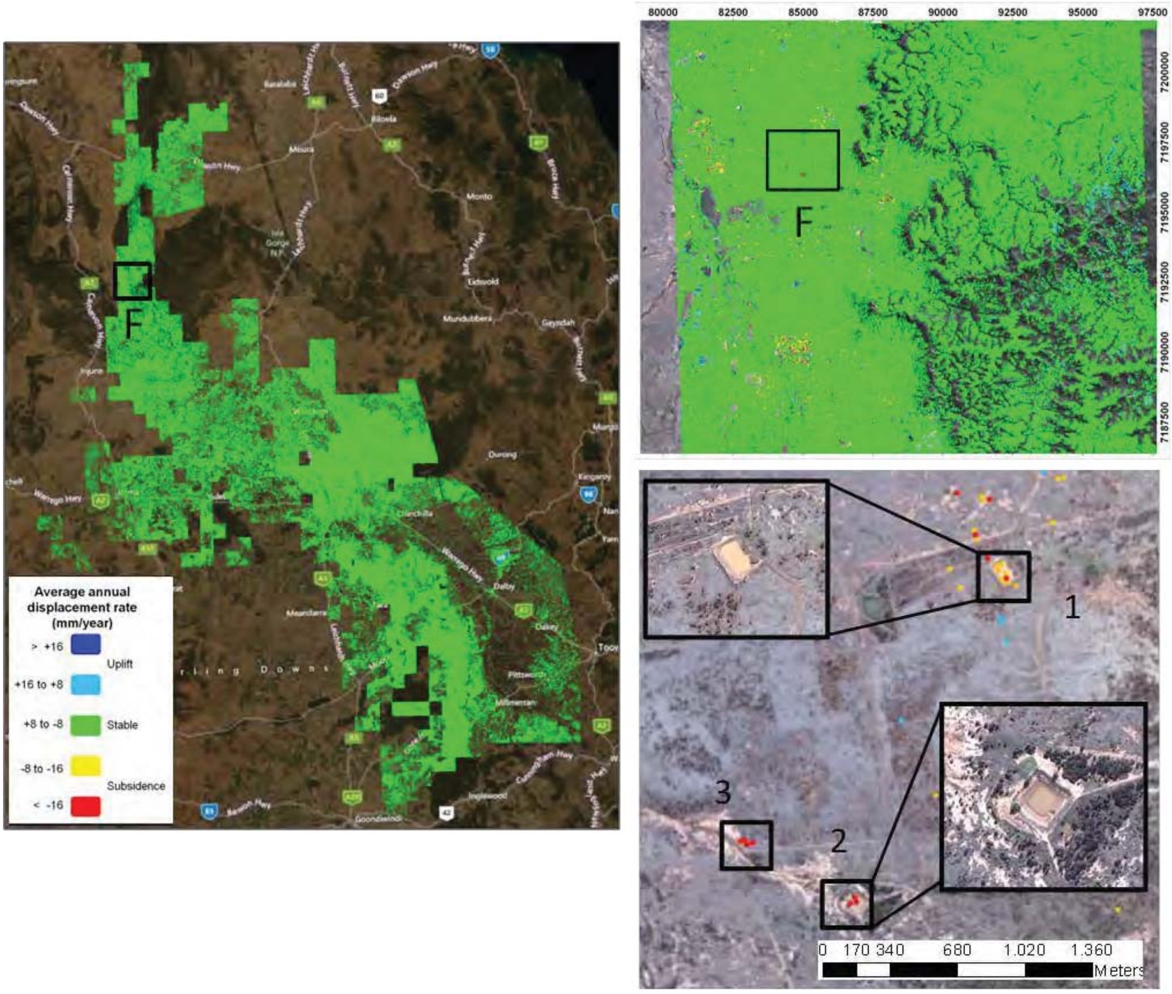

Figure 30 : Location and spatial extent of motion area F affected by ground motion

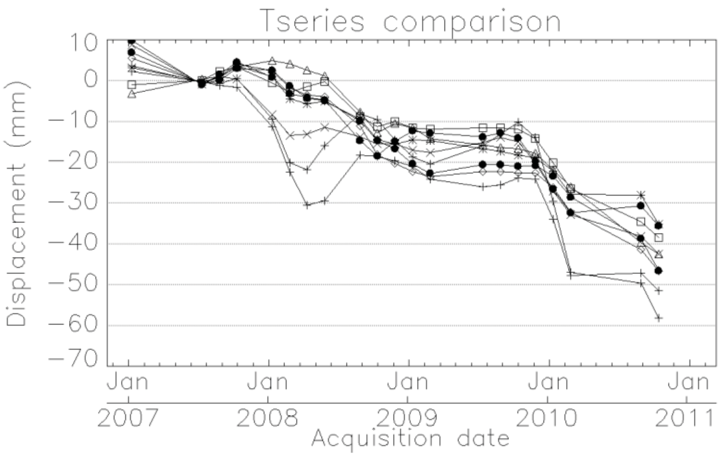

Figure 31 : Detailed time series of area F.1

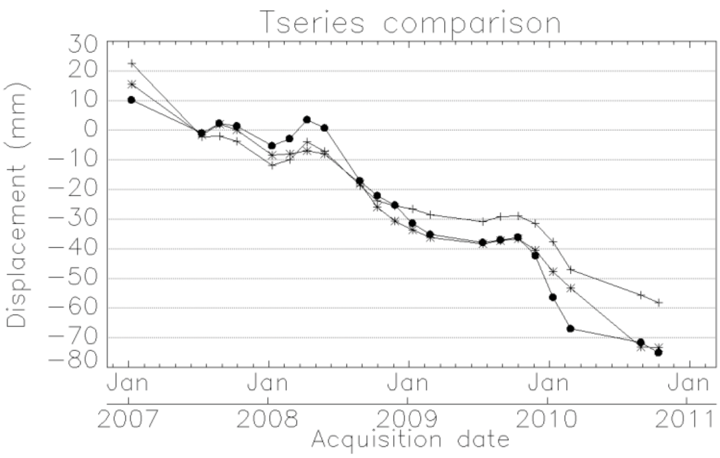

Figure 32 : Detailed time series of area F.2

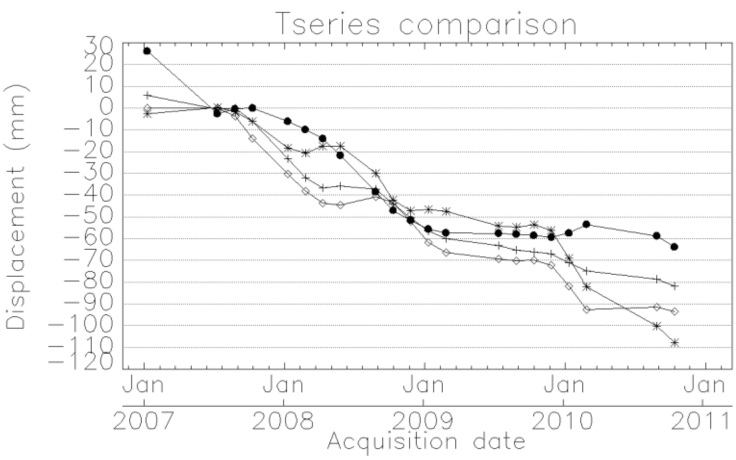

Figure 33 : Detailed time series of area F.3

APPENDIX B: RAINFALL CASE STUDY

This section explains, with the help of meteorological data, a possible correlation between some particular ground motion patterns detected by InSAR data and rainfall values. Increased rainfall values, known to have happened in 2010, might have influenced the stability of the area of study.

The annual climate statement for 2010 as reported by the Australian government Bureau of Meteorology stated that, based on preliminary numbers, 2010 was the wettest year on record for Queensland. A mean rainfall total of 690mm, well above the long-term average of 465mm, was measured. As a result, 2010 was Australia's wettest year since 2000, and the third-wettest year on record.

Figure 34 and Figure 35 present the annual rainfalls compared with historical data of the years 2009 and 2010 respectively. It can be seen that in 2009 the total rainfall is "below average" for the area of interest in this study. While in 2010 it's the "highest on record".

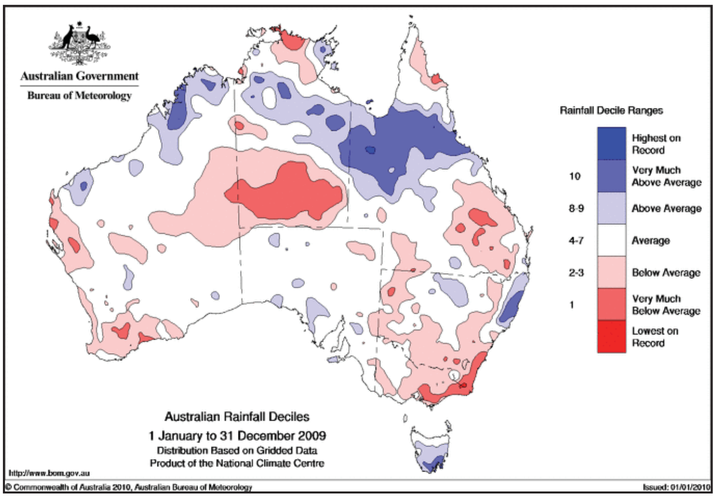

Figure 34 : 2009 annual rainfall compared against historical rainfall records. Australian Bureau of Meteorology ©

The InSAR results appear to show a systematic uplift pattern of up to 8 cm in the areas surrounding of some riverbanks, creeks and drainage lines within the study area. The analysis of the time series data plots over those areas highlight that uplift has resulted in an increase in the accumulated motion reported for 2010, which could be correlated with the reported large rainfalls over this region.

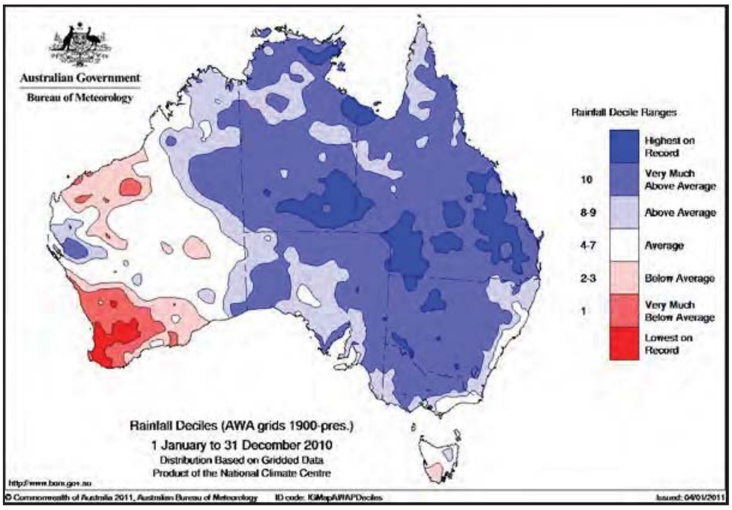

Figure 35 : 2010 annual rainfall compared against historical rainfall records. Australian Bureau of Meteorology ©

To examine the impact of rainfall on surface features further a small case study has been completed in an area around Taroom, southeast Queensland. The following images show the possible detection of flooding in the area when related to pre flood conditions and published flood plain maps.

Figure 36 shows a map of flood plain areas in and around Taroom which are delimited by the white line. Next, Figure 37 shows two time series datasets of measurements made over this area (top image). Both time series sets show stability in the period prior to 2010 (circled area) and then an increase in accumulated ground motion in 2010. Along with the graph, a map with the total accumulated magnitude of ground motion prior to the rainfall events of 2010 is presented (bottom image) to show the stability of the area before this period.

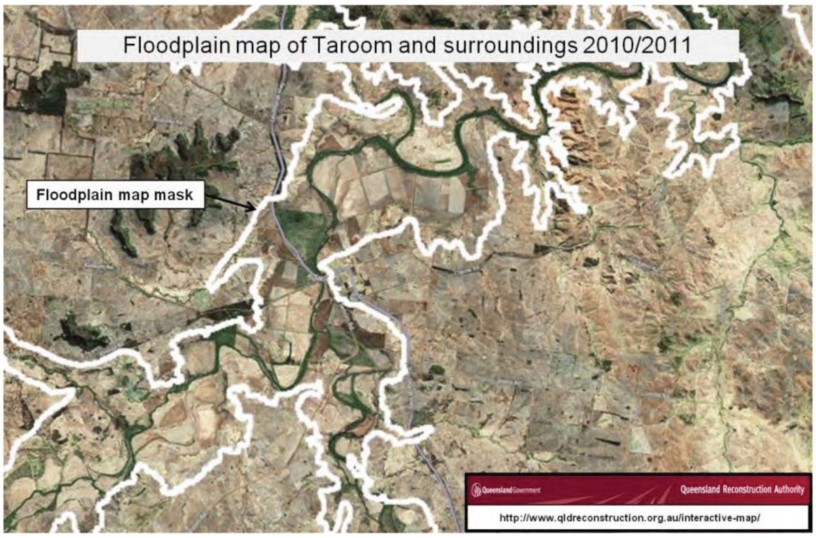

Figure 36 : Floodplain map of Taroom and surroundings (2010/2011)

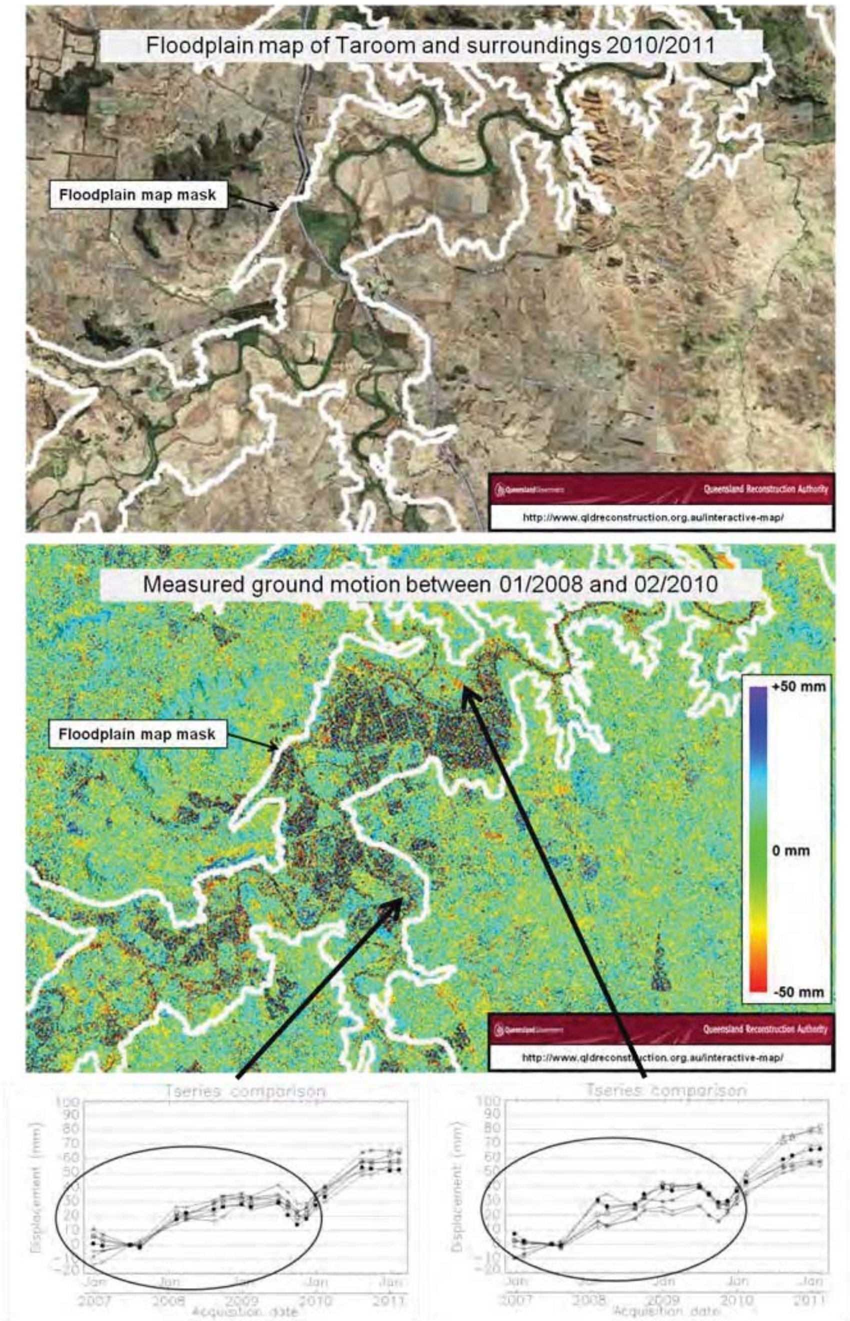

Figure 37 : Obtained InSAR results and time series over Taroom for the period between January 2008 and February 2010, period that corresponds to the circled area of the time series

Figure 38 shows the final map of the accumulated motion of 2010 (bottom image), which show the spatial extension of this abrupt uplift. The time series for this period (circled area) highlight this clear increase in the accumulated motion of up to 5cm. As it can be observed there is a correlation of the floodplain map with the areas with uplift in 2010, which could indicate a possible relationship between the heavy rains and the detected ground motion over these areas.

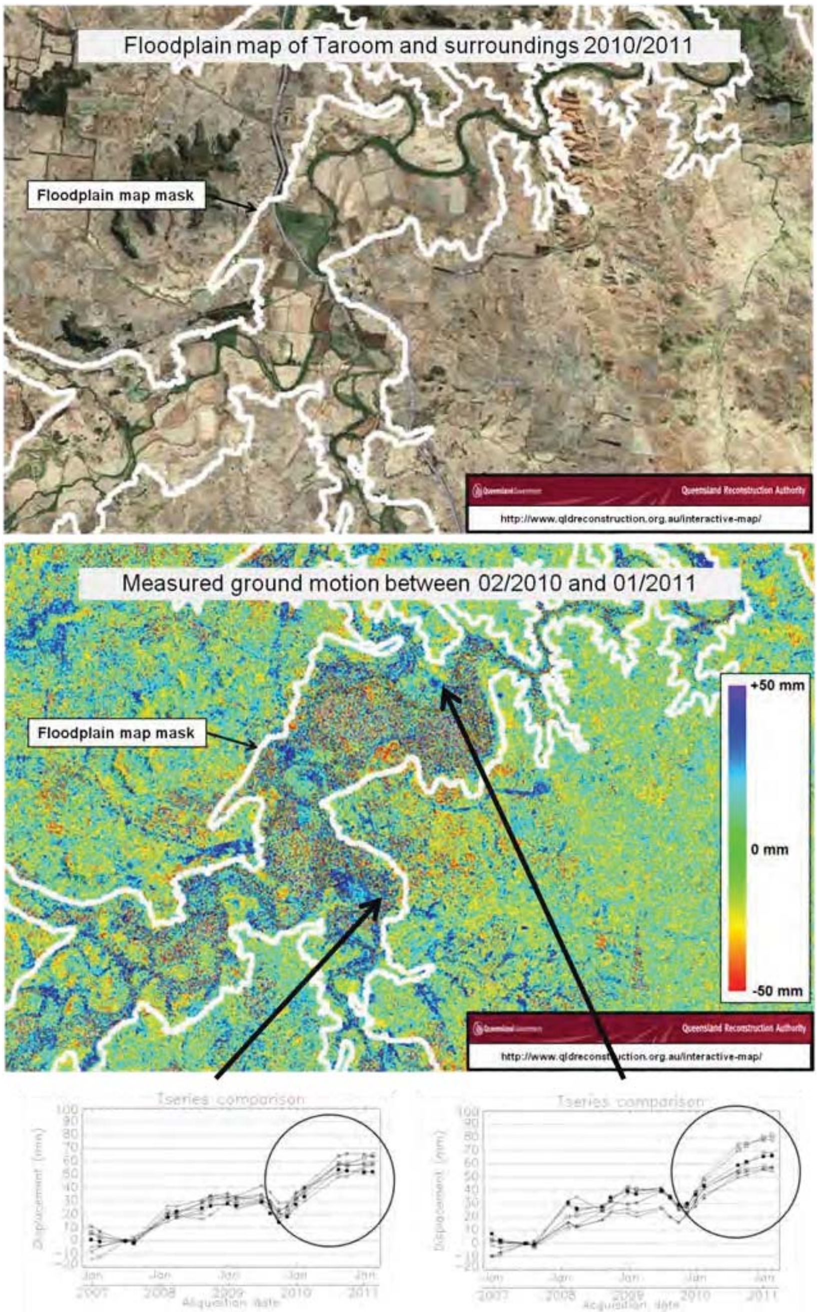

Figure 38 : Obtained InSAR results and time series over Taroom for the period between February 2010 and January 2011, period that corresponds to the circled area of the time series

APPENDIX C: MEASUREMENTS DENSITY AND DISTRIBUTION

The objective of this section is to analyse the location and the density of the measurement points. The aim is to give a qualitative justification of the uneven distribution of the measurement points in some particular areas within the AOI, especially over agricultural fields.

It is important to bear in mind that the critical factor in determining whether a measurement point can be used is whether the ground surface remains invariant during the considered period of study. In agricultural and highly vegetated areas, seasonal changes occur. Those changes also influence the distribution of the measurement points detected by the SPN software. There are also some other parameters that impact the final density and distribution of the measurements, such as the image/sensor characteristics (wavelength of the SAR signal, incidence angle, image resolution, number of available images, etc.) and the dielectric properties and roughness of the elements over the ground surface (sand, rocks, buildings and infrastructures, water, vegetation, etc.).

Figure 39 shows the location and the density of the measurement points over a sector of the area of interest. For this area, the distribution of the points is more heterogeneous as they are concentrated in particular areas where there are few changes of the land cover.

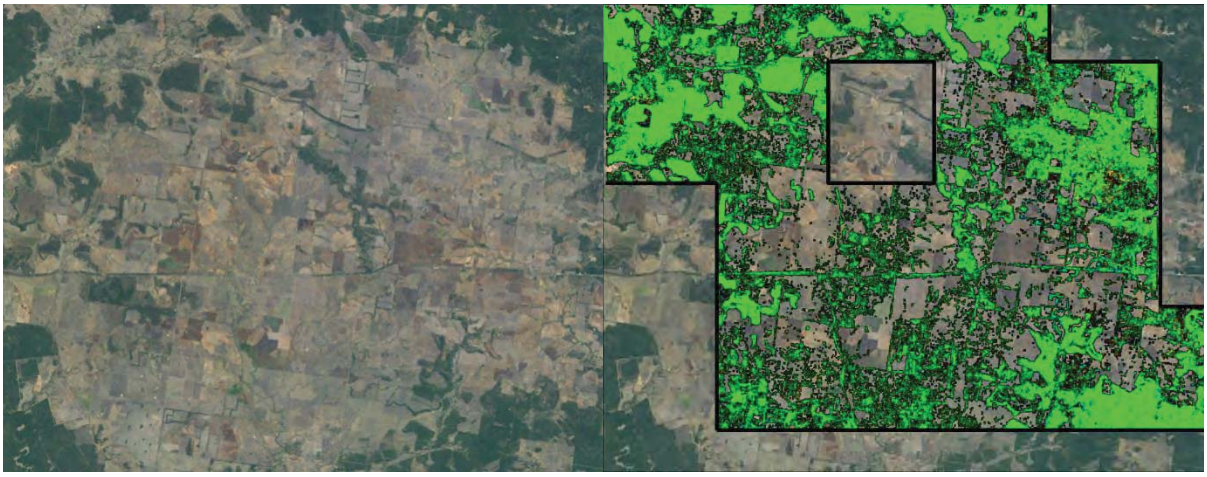

Figure 39: Orthophoto showing the land cover over a sector of the area of interest (left image) and measurement points distribution (right image). Black lines mark the limits of the delivered data

It can be seen that the areas where the measurements density is low are predominantly composed of agricultural fields. To demonstrate this situation, a land use map of the same area is presented in Figure 40. The maps were obtained through the National Dynamic Land Cover Dataset of Australia from the Australian Bureau of Agricultural and Resource Economics and Sciences © webpage.

Land use maps can help understand the distribution of the measurements since they illustrate which areas undergo changes by human interaction (ploughing, irrigation and agricultural activities). However this information must be used with care as the land use does not determine the final density of points alone. As shown in Figure 40 measurement points can be retrieved in the boundaries between crop fields or even in the middle of the fields where some small infrastructure can be present.

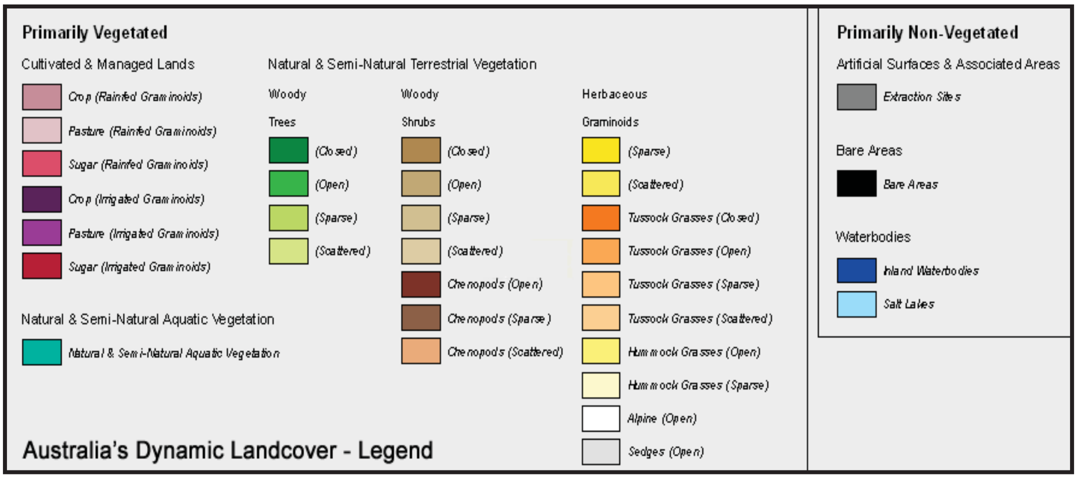

Figure 40 : Land use map from the National Dynamic Land Cover Dataset of Australia over a sector of the area of interest (top left image), measurement points distribution (top right image) and the land use map legend (lower image). Australian Bureau of Agricultural and Resource Economics and Sciences ©.

C.1 ANALYSIS OF WAVE REFLECTIVITY CHANGES OVER FIELDS

This section discusses observed changes in the signal reflectivity over fields in many sectors of the area of study. Repeated reflection changes in the SAR signal are caused by surface variations that reduce the measurements coherence over the areas that undergo these changes. This situation makes it difficult to obtain valid measurements over these mentioned sectors, and results in a notable decrease in the PS density of some of the study areas.

Figure 41 shows the SAR signal amplitude evolution in time of a specific field (red square area). The wave backscatter remains constant for the first two years of the study (from 05/12/2006 until 10/12/2008). Afterwards, a clear increase in the wave amplitude since 28/07/2009 can be seen, which means that a strong change has occurred in that field. Unfortunately, the origin of these changes cannot be given with InSAR data alone. Ancillary data (like high resolution orthophotos before and after the change) or in-situ observations are required to make further interpretations of those changes.

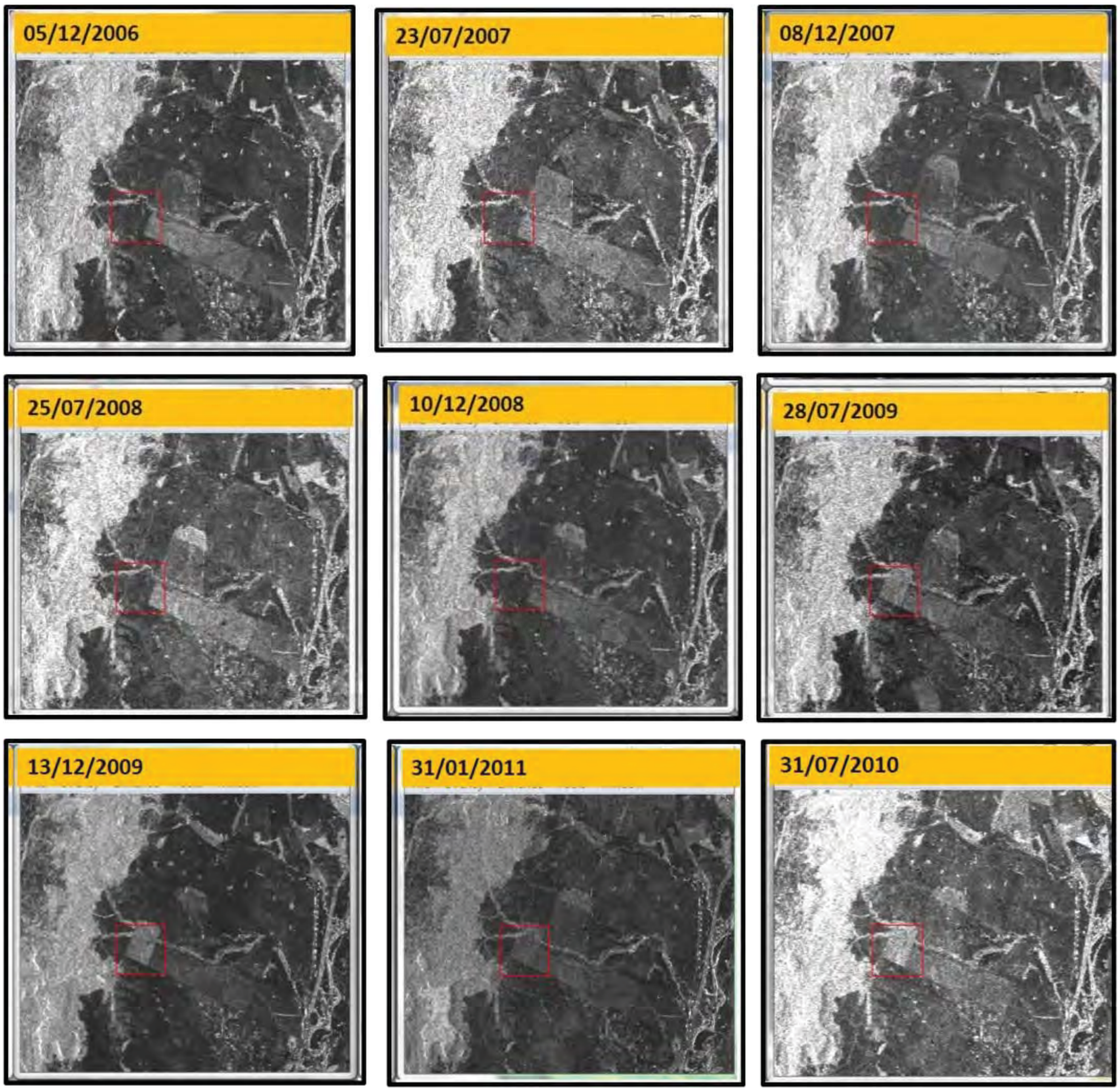

Figure 41 : Time evolution of the SAR image amplitude over a field

This change of reflectivity indicates that the SAR signal characteristics do not remain constant for the whole time period. In consequence the measurements are noisy and the final density of points is decreased. Figure 42 shows the final density of measurements over the previous field (now marked with a white rectangle) retrieved by SPN. As it can be observed the density of points is very low over this particular field with respect to the others.

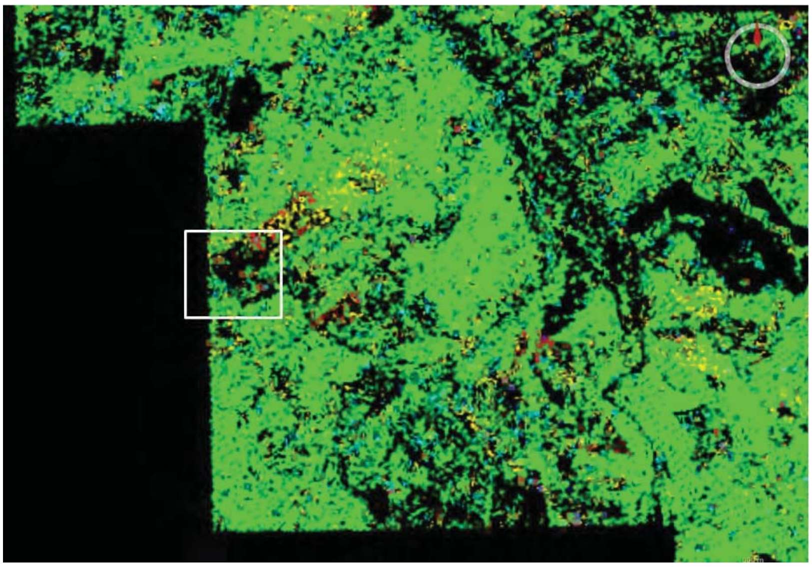

Figure 42 : Mean annual displacement map over a field presenting constant changes in the wave reflectance